

Joint association and classification analysis of multi-view data

Yunfeng Zhang* and Irina Gaynanova†

Abstract

Multi-view data, that is matched sets of measurements on the same subjects, have become increasingly common with technological advances in genomics and other fields. Often, the subjects are separated into known classes, and it is of interest to find associations between the views that are related to the class membership. Existing classification methods can either be applied to each view separately, or to the concatenated matrix of all views without taking into account between-views associations. On the other hand, existing association methods can not directly incorporate class information. In this work we propose a framework for Joint Association and Classification Analysis of multi-view data (JACA). We support the methodology with theoretical guarantees for estimation consistency in high-dimensional settings, and numerical comparisons with existing methods. In addition to joint learning framework, a distinct advantage of our approach is its ability to use partial information: it can be applied both in the settings with missing class labels, and in the settings with missing subsets of views. We apply JACA to colorectal cancer data from The Cancer Genome Atlas project, and quantify the association between RNAseq and miRNA views with respect to consensus molecular subtypes of colorectal cancer.

Keywords: Canonical correlation analysis; Data integration; Discriminant analysis; Semi-supervised learning; Sparsity; Variable selection.

*Yunfeng Zhang is PhD Student, Department of Statistics, Texas A&M University, email: yfzhang@stat.tamu.edu

†Irina Gaynanova is Assistant Professor, Department of Statistics, Texas A&M University, email: irinag@stat.tamu.edu

1 Introduction

Multi-view data, that is matched sets of measurements on the same subjects, have become increasingly common with technological advances in genomics and other fields. For example, The Cancer Genome Atlas Project (Weinstein et al., 2013) contains multiple views for the same set of subjects, such as gene expression, genotype, metabolic measurements, etc. At the same time, the subjects are often separated into known classes. For example, the breast cancer patients are typically separated into Basal, HER2, Luminal A and Luminal B subtypes (TCGA Network, 2012). Since each view presents complementary information regarding the subject’s biological system, it is of interest to answer two questions: (1) how to predict the cancer subtype given information from multiple views? (2) what are the associations between the views that are relevant for subtype prediction?

In the case of one view, the subtype prediction can be done using one of the many classification methods such as multinomial regression, multi-class support vector machines, discriminant analysis, etc. In case of multiple views, however, one has to either apply the chosen method separately to each view, or apply the method to the concatenated matrix of views. The separate approach may lead to inconsistent classification results across views. The concatenation approach ignores heterogeneity between the views in terms of scale and the number of measurements. Moreover, when one view has a much stronger subtype-specific signal, the concatenation may mask the less-dominant signals in other views. This is supported by our numerical results in Section 7.

To answer the second question, a line of research has focused on finding associations between the views based on canonical correlation analysis (Chen et al., 2013; Gao et al., 2017; Witten et al., 2009). These methods, however, do not use subtype information. Witten and Tibshirani (2009) propose supervised canonical correlation analysis, however the method is designed for the continuous response rather than the discrete class assignment, and only uses the response to filter relevant measurements. Another strategy based on factor models is proposed by Li and Jung (2017), who decompose each views into shared and individual structures that are informed by covariates. Both Witten and Tibshirani (2009) and Li and Jung (2017) use subtype information indirectly, and are not tailored towards classification.

Recently, several methods have combined the task of finding associations between the views with the task of learning the regression coefficients. Gross and Tibshirani (2015) propose to combine canonical correlation analysis with linear regression. The method, however, is restricted to univariate continuous response and can only be applied to two views. Luo et al. (2016) propose to combine canonical correlation analysis objective with a general class of loss functions. Unlike Gross and Tibshirani (2015), the method could be applied to more than two views, and binary response. Nevertheless, the method is not suited for multi-group classification, has nonconvex optimization objective and requires rank pre-specification for model fitting. Finally, neither Gross and Tibshirani (2015) nor Luo et al. (2016) discuss the underlying population model, and the methods come with no theoretical guarantees.

In this work, we develop a framework for Joint Association and Classification Analysis (JACA) of multi-view data by connecting discriminant analysis with canonical correlation analysis. Since the method of Luo et al. (2016) also allows to perform joint association

and classification in the two-class case, we further contrast two approaches. First, we use discriminant analysis rather than the regression framework, which allows us to fix the rank for model fitting to be $K - 1$, where K is the number of classes. In Luo et al. (2016), the rank of the model has to be chosen by the user. Secondly, we are able to formulate our method as a convex optimization problem by using the optimal scoring formulation of multi-class discriminant analysis (Hastie et al., 1994) and fixing the scores to be orthogonally invariant (Gaynanova, 2018). We add group-lasso type penalty to the optimization objective to allow for variable selection, and use block-coordinate descent algorithm to solve the corresponding convex problem. In contrast, the method of Luo et al. (2016) is nonconvex, and requires the use of variable splitting and augmented Lagrangian. Finally, we provide theoretical guarantees on the estimation consistency of JACA which are absent for previously proposed joint learning methods (Luo et al., 2016; Gross and Tibshirani, 2015).

While estimation consistency has been established separately for discriminant analysis (Li and Jia, 2017; Gaynanova, 2018) and canonical correlation analysis (Gao et al., 2017), providing similar guarantees for JACA is not straightforward due to the unique structure of our framework. We use the augmented data approach to rewrite our method as a penalized linear regression problem, and use sub-exponential concentration bounds to control the inner-product between the augmented random design matrix and the random matrix of residuals. Despite the dependency between corresponding design matrix and the matrix of residuals, we obtain the estimation error bound that is of the same order as the known bounds for group-lasso linear regression (Lounici et al., 2011; Nardi and Rinaldo, 2008).

Another advantage of the proposed method is that it can be extended to the multi-view data with block-missing structure, that is to cases where a subset of views or class labels is missing for some subjects. In Section 7 we consider colorectal cancer data, where out of 282 subjects with RNAseq data, only 167 subjects have corresponding miRNA and cancer subtype information. While most methods can only use data from 167 subjects with complete information, our approach can utilize data from 78 extra subjects for which at least two types of information are available (two views with no class labels, or class labels with only one view). Section 6 shows an improved estimation performance of JACA when the subjects with incomplete information are added to the analysis.

In summary, this work has four main contributions. First, we establish a connection between discriminant analysis and canonical correlation analysis via the factor model. Secondly, we use this connection to formulate the JACA method for Joint Classification and Association Analysis via convex optimization problem. Third, we provide finite sample bounds on estimation consistency of our method in high-dimensional settings. Finally, we generalize our approach to the settings with block-missing data without the use of imputation.

The rest of the paper is organized as follows. Section 2 establishes the connection between canonical correlation analysis and linear discriminant analysis, and describes the proposed JACA method. Section 3 provides the estimation error bound in high-dimensional settings. Section 4 describes the method’s implementation. Section 5 describes generalization of JACA to block-missing data. Section 6 provides numerical comparisons with other methods on simulated data. Section 7 provides the analysis of colorectal cancer data from The Cancer

Genome Atlas project. Section 8 concludes with discussion. The technical proofs of the main results, and additional numerical studies are deferred to Appendix.

2 Proposed methodology

2.1 Notation

We consider n independent observations $(\mathbf{x}_{1i}, \dots, \mathbf{x}_{di}, y_i) \in \mathbb{R}^{p_1} \times \dots \times \mathbb{R}^{p_d} \times \{1, \dots, K\}$, where \mathbf{x}_{di} is the i th sample's measurements from view d , and y_i is the corresponding class assignment. For two scalars $a, b \in \mathbb{R}$, we let $a \vee b = \max(a, b)$. For a vector $\mathbf{v} \in \mathbb{R}^p$, we let $\|\mathbf{v}\|_2 = (\sum_{j=1}^p v_j^2)^{1/2}$, $\|\mathbf{v}\|_1 = \sum_{j=1}^p |v_j|$ and $\|\mathbf{v}\|_\infty = \max_j |v_j|$. For matrices $\mathbf{M}, \mathbf{N} \in \mathbb{R}^{n \times p}$, we let $\|\mathbf{M}\|_F = (\sum_{i=1}^n \sum_{j=1}^p m_{ij}^2)^{1/2}$, $\|\mathbf{M}\|_{\infty,2} = \max_{1 \leq i \leq n} (\sum_{j=1}^p m_{ij}^2)^{1/2}$, $\|\mathbf{M}\|_{1,2} = \sum_{i=1}^n (\sum_{j=1}^p m_{ij}^2)^{1/2}$ and $\langle \mathbf{M}, \mathbf{N} \rangle = \text{Tr}(\mathbf{M}^\top \mathbf{N})$. We use $\mathbf{I} = \mathbf{I}_p$ to denote $p \times p$ identity matrix, and $\mathbf{0}$ to denote zero matrix. For two sequences of scalars a_1, \dots, a_n, \dots and b_1, \dots, b_n, \dots , we use $b_n = o(a_n)$ if $\lim_{n \rightarrow \infty} (b_n/a_n) = 0$ and $b_n = O(a_n)$ if $\lim_{n \rightarrow \infty} (b_n/a_n) = C$ for some finite constant C . For two sequences of random variables x_1, \dots, x_n, \dots and y_1, \dots, y_n, \dots , we use $y_n = o_p(x_n)$ if for any $\varepsilon > 0$ $P(|y_n/x_n| < \varepsilon) \rightarrow 0$ as $n \rightarrow \infty$, and $y_n = O_p(x_n)$ if for any $\varepsilon > 0$ there exists M_ε such that $P(|y_n/x_n| > M_\varepsilon) < \varepsilon$ for all n .

2.2 Connection between canonical correlation and linear discriminant analysis

In this section, we review the canonical correlation analysis (CCA) and the linear discriminant analysis (LDA). We demonstrate that discriminant vectors in LDA coincide with the subset of canonical vectors in CCA, and use this connection to motivate the proposed method.

Consider two mean zero random vectors $\mathbf{x}_1 \in \mathbb{R}^{p_1}$ and $\mathbf{x}_2 \in \mathbb{R}^{p_2}$ with $\Sigma_1 = \mathbb{E}(\mathbf{x}_1 \mathbf{x}_1^\top)$, $\Sigma_2 = \mathbb{E}(\mathbf{x}_2 \mathbf{x}_2^\top)$, $\Sigma_{12} = \mathbb{E}(\mathbf{x}_1 \mathbf{x}_2^\top)$ and $r = \text{rank}(\Sigma_{12}) > 0$. The population CCA seeks linear combinations $(\boldsymbol{\theta}_1, \boldsymbol{\theta}_2)$ that maximize $\text{Cor}(\boldsymbol{\theta}_1^\top \mathbf{x}_1, \boldsymbol{\theta}_2^\top \mathbf{x}_2)$, that is it seeks at most r pairs $(\boldsymbol{\theta}_1^{(k)}, \boldsymbol{\theta}_2^{(k)})$ that satisfy

$$\begin{aligned} (\boldsymbol{\theta}_1^{(k)}, \boldsymbol{\theta}_2^{(k)}) &= \underset{\mathbf{w}_1^{(k)}, \mathbf{w}_2^{(k)}}{\text{argmax}} \left\{ \mathbf{w}_1^{(k)\top} \Sigma_{12} \mathbf{w}_2^{(k)} \right\} \\ \text{subject to } & \mathbf{w}_1^{(k)\top} \Sigma_1 \mathbf{w}_1^{(k)} = 1, \mathbf{w}_2^{(k)\top} \Sigma_2 \mathbf{w}_2^{(k)} = 1, \\ & \mathbf{w}_1^{(k)\top} \Sigma_1 \mathbf{w}_1^{(j)} = 0, \mathbf{w}_2^{(k)\top} \Sigma_2 \mathbf{w}_2^{(j)} = 0 \quad \text{for } j < k. \end{aligned}$$

The pairs $(\boldsymbol{\theta}_1^{(k)}, \boldsymbol{\theta}_2^{(k)})$ are called canonical vectors, and the values $\rho_k = \boldsymbol{\theta}_1^{(k)\top} \Sigma_{12} \boldsymbol{\theta}_2^{(k)}$ are canonical correlations. By definition, $1 \geq \rho_1 \geq \rho_2 \geq \dots \geq \rho_r > 0$ and $\left\{ \boldsymbol{\theta}_d^{(k)} \right\}_{k=1}^r$ are orthonormal with respect to Σ_d , $\boldsymbol{\theta}_d^{(i)\top} \Sigma_d \boldsymbol{\theta}_d^{(j)} = \mathbb{1}\{i = j\}$. Moreover, the population CCA problem can be equivalently formulated as the matrix decomposition problem of Σ_{12} , that

is the r pairs $(\boldsymbol{\theta}_1^{(k)}, \boldsymbol{\theta}_2^{(k)})$ solve the population CCA problem if and only if (Chen et al., 2013)

$$\boldsymbol{\Sigma}_{12} = \boldsymbol{\Sigma}_1 \left(\sum_{k=1}^r \rho_k \boldsymbol{\theta}_1^{(k)} \boldsymbol{\theta}_2^{(k)\top} \right) \boldsymbol{\Sigma}_2. \quad (1)$$

This alternative formulation of CCA proves useful in drawing connections with LDA.

Consider a random variable y indicating the class assignment such that $P(y = k) = \pi_k$ for $k = 1, \dots, K$. Consider mean zero random vectors $\boldsymbol{x}_d \in \mathbb{R}^{p_d}$, $d \in \{1, \dots, D\}$, with class-conditional means and covariance matrices specified as

$$\mathbb{E} \left[\begin{pmatrix} \boldsymbol{x}_1 \\ \vdots \\ \boldsymbol{x}_D \end{pmatrix} \middle| y = k \right] = \begin{pmatrix} \boldsymbol{\mu}_{1k} \\ \vdots \\ \boldsymbol{\mu}_{Dk} \end{pmatrix}, \quad \text{Cov} \left[\begin{pmatrix} \boldsymbol{x}_1 \\ \vdots \\ \boldsymbol{x}_D \end{pmatrix} \middle| y = k \right] = \boldsymbol{\Sigma}_y = \begin{pmatrix} \boldsymbol{\Sigma}_{1y} & \dots & \boldsymbol{\Sigma}_{1Dy} \\ & \ddots & \\ \boldsymbol{\Sigma}_{1Dy}^\top & \dots & \boldsymbol{\Sigma}_{Dy} \end{pmatrix}, \quad (2)$$

where we assume that the covariance matrices are equal between the groups as in LDA (we keep subscript y to differentiate class-conditional covariance matrix $\boldsymbol{\Sigma}_y$ from marginal covariance matrix $\boldsymbol{\Sigma}$). We next show that under additional assumptions on $\boldsymbol{\Sigma}_y$, the class-conditional specification (2) is equivalent to the factor model.

Proposition 1. *Let y be a random variable with $P(y = k) = \pi_k$, $k = 1, \dots, K$, and let $\boldsymbol{x}_d \in \mathbb{R}^{p_d}$ be mean-zero random vectors with class-conditional specification (2). Further, let $\boldsymbol{\Sigma}_{ldy} = \mathbf{0}$ for all $l \neq d \in \{1, \dots, D\}$. Then each \boldsymbol{x}_d can be equivalently specified via the factor model:*

$$\boldsymbol{x}_d = \boldsymbol{\mu}_d + \boldsymbol{\Delta}_d \boldsymbol{u}_y + \boldsymbol{\Sigma}_{dy}^{1/2} \boldsymbol{e}_d, \quad (3)$$

where $\boldsymbol{\mu}_d = \mathbf{0}$ is the overall mean; $\boldsymbol{u}_y = f(y) \in \mathbb{R}^{K-1}$ is a random vector indicating class assignment with $\mathbb{E}(\boldsymbol{u}_y) = \mathbf{0}$, $\text{Cov}(\boldsymbol{u}_y) = \mathbf{I}$; $\boldsymbol{\Delta}_d \in \mathbb{R}^{p_d \times (K-1)}$ is such that $\boldsymbol{\Delta}_d^\top \boldsymbol{\Sigma}_{dy}^{-1} \boldsymbol{\Delta}_d = \boldsymbol{\Lambda}_d$ is diagonal with $\mathbb{E}(\boldsymbol{\mu}_d + \boldsymbol{\Delta}_d \boldsymbol{u}_y | y = k) = \boldsymbol{\mu}_{dk}$; $\boldsymbol{\Sigma}_{dy}$ is class-conditional covariance matrix for view d , and $\boldsymbol{e}_d \in \mathbb{R}^{p_d}$ are independent from y isotropic noise vectors.

Remark 1. *If $\text{rank}(\boldsymbol{\Delta}_d^\top \boldsymbol{\Sigma}_{dy}^{-1} \boldsymbol{\Delta}_d) = r < K - 1$, then (3) is not identifiable as the effective number of class-specific factors r is less than $K - 1$. For clarity, we assume throughout that $r = K - 1$, but the results can be generalized at the expense of a more technical proof. When $K = 2$, the restriction is equivalent to requiring the class-conditional means to be distinct.*

The factor model (3) is directly connected with discriminant vectors in LDA. When $K > 2$, Gaynanova et al. (2016) show that the matrix of discriminant vectors can be expressed as $\boldsymbol{W}_d \propto \boldsymbol{\Sigma}_d^{-1} \boldsymbol{\Delta}_d$, where \propto is applied columnwise. Hence, by fixing the magnitude of discriminant vectors in accordance with (3), we can rewrite the factor model as

$$\boldsymbol{x}_d = \boldsymbol{\mu}_d + \boldsymbol{\Sigma}_{dy} \boldsymbol{W}_d \boldsymbol{u}_y + \boldsymbol{\Sigma}_{dy}^{1/2} \boldsymbol{e}_d,$$

where $\boldsymbol{W}_d^\top \boldsymbol{\Sigma}_{dy} \boldsymbol{W}_d$ is a diagonal matrix. This representation allows to treat the matrix of discriminant vectors \boldsymbol{W}_d as a covariance-adjusted matrix of loadings in the above factor

model. The main limitation of Proposition 1, however, is the requirement $\Sigma_{ldy} = \mathbf{0}$, that is the assumption that \mathbf{u}_y are the only common factors between the views.

To consider a more general case with $\Sigma_{ldy} \neq \mathbf{0}$, we adjust the factor model (3) as

$$\mathbf{x}_d = \boldsymbol{\mu}_d + \boldsymbol{\Delta}_d \mathbf{u}_y + \mathbf{A}_d \mathbf{u} + \tilde{\Sigma}_d^{1/2} \mathbf{e}_d, \quad (4)$$

where $\boldsymbol{\mu}_d$, $\boldsymbol{\Delta}_d$, \mathbf{u}_y are as in Proposition 1, $\mathbf{u} \in \mathbb{R}^q$ is a random vector independent of y representing q extra common factors between the D views with $\mathbb{E}(\mathbf{u}) = \mathbf{0}$, $\text{Cov}(\mathbf{u}) = \mathbf{I}$, and $\mathbf{e}_d \in \mathbb{R}^{p_d}$ is an independent noise vector with $\mathbb{E}(\mathbf{e}_d) = \mathbf{0}$, $\text{Cov}(\mathbf{e}_d) = \mathbf{I}$. Here $\tilde{\Sigma}_d$ is no longer class-conditional covariance matrix, but rather covariance matrix after accounting for both class membership (\mathbf{u}_y) and other shared factors (\mathbf{u}). When $\mathbf{A}_d = \mathbf{0}$, the model reduces to (3). We assume \mathbf{A}_d is full rank given q (with $\mathbf{A}_d = \mathbf{0}$ for $q = 0$). Rewriting (4) as

$$\tilde{\Sigma}_d^{-1/2} \mathbf{x}_d = \tilde{\Sigma}_d^{-1/2} \boldsymbol{\mu}_d + \tilde{\Sigma}_d^{-1/2} \boldsymbol{\Delta}_d \mathbf{u}_y + \tilde{\Sigma}_d^{-1/2} \mathbf{A}_d \mathbf{u} + \mathbf{e}_d,$$

we further assume that each loadings matrix $\mathbf{V}_d = [\tilde{\Sigma}_d^{-1/2} \boldsymbol{\Delta}_d \tilde{\Sigma}_d^{-1/2} \mathbf{A}_d] \in \mathbb{R}^{p_d \times (K-1+q)}$ is orthogonal following standard identifiability conditions for factor models (Mardia et al., 1979, Chapter 9.2). As with model (3), we can rewrite (4) in terms of view-specific discriminant vectors as

$$\mathbf{x}_d = \boldsymbol{\mu}_d + \tilde{\Sigma}_d \mathbf{W}_d \mathbf{u}_y + \mathbf{A}_d \mathbf{u} + \tilde{\Sigma}_d^{1/2} \mathbf{e}_d.$$

We next connect the LDA-based factor model (4) with the CCA decomposition (1).

Theorem 1. *Consider the factor model (4) with corresponding identifiability conditions. Let $\Sigma_{ld} = \mathbb{E}(\mathbf{x}_l \mathbf{x}_d^\top)$ be the corresponding marginal cross-covariance matrix between mean zero \mathbf{x}_l and \mathbf{x}_d .*

1. *If $q = 0$, (4) reduces to (3) and*

$$\Sigma_{ld} = \Sigma_l \left(\sum_{k=1}^{K-1} \rho_k \boldsymbol{\theta}_l^{(k)} \boldsymbol{\theta}_d^{(k)\top} \right) \Sigma_d,$$

where $\boldsymbol{\Theta}_d = [\boldsymbol{\theta}_d^{(1)} \dots \boldsymbol{\theta}_d^{(K-1)}] \propto \Sigma_d^{-1} \boldsymbol{\Delta}_d$ is orthonormal with respect to Σ_d , and ρ_k are diagonal elements of matrix $(\mathbf{I} + \boldsymbol{\Lambda}_l)^{-1/2} \boldsymbol{\Lambda}_l^{1/2} \boldsymbol{\Lambda}_d^{1/2} (\mathbf{I} + \boldsymbol{\Lambda}_d)^{-1/2}$.

2. *If $q > 0$,*

$$\Sigma_{ld} = \Sigma_l \left(\sum_{k=1}^{q+K-1} \rho_k \boldsymbol{\theta}_l^{(k)} \boldsymbol{\theta}_d^{(k)\top} \right) \Sigma_d,$$

where $\left\{ \boldsymbol{\theta}_d^{(k)} \right\}_{k=1}^{q+K-1}$ are orthonormal with respect to Σ_d , $\Sigma_l \left(\sum_{k=1}^q \rho_k \boldsymbol{\theta}_1^{(k)} \boldsymbol{\theta}_2^{(k)\top} \right) \Sigma_d = \mathbf{A}_l \mathbf{A}_d^\top$ and $\Sigma_l \left(\sum_{k=q+1}^{q+K-1} \rho_k \boldsymbol{\theta}_1^{(k)} \boldsymbol{\theta}_2^{(k)\top} \right) \Sigma_d = \boldsymbol{\Delta}_l \boldsymbol{\Delta}_d^\top$ are as in part 1.

If $q = 0$, then the only relationship between the views is due to shared class membership (\mathbf{u}_y). In this case, the canonical vectors Θ_d in CCA coincide with discriminant vectors \mathbf{W}_d in LDA. If $q > 0$, then there exists extra q factors that are shared between the views, leading to q extra pairs of canonical vectors in CCA. If the LDA directions correspond to the maximal ρ_k , then the first $K - 1$ canonical pairs coincide with discriminant vectors. If the LDA directions do not correspond to the maximal ρ_k , then the first $K - 1$ canonical pairs include other shared factors that are independent of class membership.

2.3 Joint association and classification analysis

Our goal is to estimate view-specific matrices of canonical vectors that correspond to discriminant directions in LDA, that is to estimate $\mathbf{W}_d \propto \Sigma_d^{-1} \Delta_d$. In light of correspondence between CCA and LDA explored in Theorem 1, our proposal is based on combining the strengths of both approaches. On the one hand, we want to perform well in classification. On the other hand, we want to maximize the correlation between the views.

For the classification, we reformulate sparse multi-group discriminant analysis (Gayanova et al., 2016) as penalized optimal scoring problem (Hastie et al., 1994).

Proposition 2. *Let $\mathbf{X} \in \mathbb{R}^{n \times p}$ be the column-centered data matrix, $\mathbf{Z} \in \mathbb{R}^{n \times K}$ be the corresponding class-indicator matrix, n_k be the number of samples in class k and $s_k = \sum_{i=1}^k n_i$. Let $\mathbf{H} \in \mathbb{R}^{K \times K-1}$ have columns $\mathbf{H}_l \in \mathbb{R}^K$ defined as*

$$\mathbf{H}_l = \left(\left\{ (nn_{l+1})^{1/2} (s_l s_{l+1})^{-1/2} \right\}_l, \quad -(ns_l)^{1/2} (n_{l+1} s_{l+1})^{-1/2}, \quad \mathbf{0}_{K-1-l} \right)^\top,$$

and let $\tilde{\mathbf{Y}} = \mathbf{Z}\mathbf{H}$. Then the discriminant vectors in multi-group sparse discriminant analysis (Gayanova et al., 2016) correspond to the solution of

$$\underset{\mathbf{V} \in \mathbb{R}^{p \times (K-1)}}{\text{minimize}} \left\{ \frac{1}{2n} \|\tilde{\mathbf{Y}} - \mathbf{X}\mathbf{V}\|_F^2 + \lambda \sum_{i=1}^p \|\mathbf{v}_i\|_2 \right\}. \quad (5)$$

Hence, the problem of finding sparse discriminant directions in the multi-group case can be recast as the multi-response penalized least-squares linear regression problem.

For the correlation between the views, we rewrite the sample CCA criterion for column-centered views \mathbf{X}_d and \mathbf{X}_l as minimization of the least squares objective subject to orthogonality constraints

$$\underset{\mathbf{W}_d, \mathbf{W}_l}{\text{minimize}} \|\mathbf{X}_d \mathbf{W}_d - \mathbf{X}_l \mathbf{W}_l\|_F^2 \quad \text{subject to} \quad \frac{1}{n} \mathbf{W}_d^\top \mathbf{X}_d^\top \mathbf{X}_d \mathbf{W}_d = \mathbf{I}, \quad \frac{1}{n} \mathbf{W}_l^\top \mathbf{X}_l^\top \mathbf{X}_l \mathbf{W}_l = \mathbf{I}. \quad (6)$$

We propose to find the matrices of discriminant vectors $\mathbf{W}_d \in \mathbb{R}^{p_d \times (K-1)}$ by combining

classification objective (5) with canonical correlation objective (6):

$$\begin{aligned} \underset{\mathbf{W}_1, \dots, \mathbf{W}_D}{\text{minimize}} \left\{ \frac{\alpha}{2nD} \sum_{d=1}^D \|\tilde{\mathbf{Y}} - \mathbf{X}_d \mathbf{W}_d\|_F^2 + \frac{1-\alpha}{2nD(D-1)} \sum_{d=1}^{D-1} \sum_{l=d+1}^D \|\mathbf{X}_d \mathbf{W}_d - \mathbf{X}_l \mathbf{W}_l\|_F^2 \right. \\ \left. + \sum_{d=1}^D \lambda_d \text{Pen}(\mathbf{W}_d) \right\} \quad \text{subject to} \quad \frac{1}{n} \mathbf{W}_d^\top \mathbf{X}_d^\top \mathbf{X}_d \mathbf{W}_d = \mathbf{I}, \quad \text{for } 1 \leq d \leq D. \end{aligned} \quad (7)$$

Here $\text{Pen}(\mathbf{W}_d)$ can be used to put structural assumptions on \mathbf{W}_d such as sparsity, and $\alpha \in [0, 1]$ controls the relative weights between LDA and CCA criteria. When $\alpha = 0$, (7) reduces to sparse CCA. When $\alpha = 1$, (7) reduces to sparse LDA with additional orthogonality constraints. While the orthogonality constraints are required for CCA criterion (6) to avoid trivial zero solution, they are not necessary in (8) as long as $\alpha > 0$ due to the addition of the optimal scoring loss function. Moreover, the classification rule in discriminant analysis is invariant to both scaling and orthogonal transformation of the matrix of discriminant vectors (Gaynanova et al., 2016). To make the problem convex and simplify computations, we only consider $\alpha > 0$, and drop the orthogonality constraints in (7) leading to

$$\begin{aligned} \underset{\mathbf{W}_1, \dots, \mathbf{W}_D}{\text{minimize}} \left\{ \frac{\alpha}{2nD} \sum_{d=1}^D \|\tilde{\mathbf{Y}} - \mathbf{X}_d \mathbf{W}_d\|_F^2 \right. \\ \left. + \frac{1-\alpha}{2nD(D-1)} \sum_{d=1}^{D-1} \sum_{l=d+1}^D \|\mathbf{X}_d \mathbf{W}_d - \mathbf{X}_l \mathbf{W}_l\|_F^2 + \sum_{d=1}^D \lambda_d \text{Pen}(\mathbf{W}_d) \right\}. \end{aligned} \quad (8)$$

We call (8) JACA for Joint Association and Classification Analysis, and choose convex $\text{Pen}(\mathbf{W}_d) = \sum_{i=1}^{p_d} \|\mathbf{w}_{di}\|_2$ to encourage variable selection via row-wise sparsity in \mathbf{W}_d .

Further, problem (8) can be rewritten as a multi-response linear regression problem using the augmented data approach. For simplicity, we illustrate the case $D = 2$, the more general case is described in Appendix C. Let $\mathbf{W} = (\mathbf{W}_1^\top, \mathbf{W}_2^\top)^\top$,

$$\mathbf{Y}' = \frac{\sqrt{\alpha}}{\sqrt{nD}} \begin{pmatrix} \tilde{\mathbf{Y}} \\ \mathbf{0} \end{pmatrix}, \quad \mathbf{X}' = \frac{1}{\sqrt{nD}} \begin{pmatrix} \sqrt{\alpha} \mathbf{X}_1 & \mathbf{0} \\ \mathbf{0} & \sqrt{\alpha} \mathbf{X}_2 \\ \sqrt{(1-\alpha)/(D-1)} \mathbf{X}_1 & -\sqrt{(1-\alpha)/(D-1)} \mathbf{X}_2 \end{pmatrix}.$$

Then (8) is equivalent to

$$\underset{\mathbf{W}}{\text{minimize}} \left\{ 2^{-1} \|\mathbf{Y}' - \mathbf{X}' \mathbf{W}\|_F^2 + \sum_{d=1}^D \lambda_d \text{Pen}(\mathbf{W}_d) \right\}. \quad (9)$$

3 Estimation consistency

In this section, we derive the finite sample bound on the estimation error of the minimizer of (9) with $\text{Pen}(\mathbf{W}_d) = \sum_{i=1}^{p_d} \|\mathbf{w}_{di}\|_2$. From Theorem 1, our goal is to estimate the view-specific matrices of discriminant vectors Θ_d , which are equal to $\Sigma_d^{-1} \Delta_d$ up to column scaling.

To connect (9) with Θ_d , consider the population objective function of (9) with $\lambda_d = 0$

$$\mathbb{E}(2^{-1}\|\mathbf{Y}' - \mathbf{X}'\mathbf{W}\|_F^2) = 2^{-1} \text{Tr}\{\mathbf{W}^\top \mathbb{E}(\mathbf{X}'^\top \mathbf{X}')\mathbf{W}\} - \text{Tr}\{\mathbf{W}^\top \mathbb{E}(\mathbf{X}'^\top \mathbf{Y}')\} + C, \quad (10)$$

where C is a constant independent of \mathbf{W} . Using the definition of augmented \mathbf{X}' and \mathbf{Y}' ,

$$\mathbb{E}(\mathbf{X}'^\top \mathbf{X}') = \begin{pmatrix} \Sigma_1 & -\frac{1-\alpha}{D-1}\Sigma_{12} & \cdots & -\frac{1-\alpha}{D-1}\Sigma_{1D} \\ -\frac{1-\alpha}{D-1}\Sigma_{21} & \Sigma_2 & \cdots & -\frac{1-\alpha}{D-1}\Sigma_{2D} \\ \vdots & \vdots & \ddots & \vdots \\ -\frac{1-\alpha}{D-1}\Sigma_{D1} & -\frac{1-\alpha}{D-1}\Sigma_{D2} & \cdots & \Sigma_D \end{pmatrix} / D := \mathbf{G},$$

and using Lemma 8 in Gaynanova and Kolar (2015) for the r th column of $\mathbf{X}'^\top \mathbf{Y}'$

$$\mathbb{E}(\mathbf{X}'^\top \mathbf{Y}'_r) = \frac{\alpha}{D} \mathbb{E}\left\{\frac{1}{n}(\mathbf{X}'_1^\top \tilde{\mathbf{Y}}_r \cdots \mathbf{X}'_D^\top \tilde{\mathbf{Y}}_r)^\top\right\} = \tilde{\Delta}_r + o(1).$$

Here $o(1)$ term captures the differences between empirical class proportions n_k/n and prior class probabilities π_k , and $\tilde{\Delta} \in \mathbb{R}^{(\sum_{i=1}^D p_i) \times (K-1)}$ has r th column defined as

$$\tilde{\Delta}_r = \frac{\alpha}{D} \frac{\sqrt{\pi_{r+1}} \sum_{k=1}^r \pi_k (\boldsymbol{\mu}_k - \boldsymbol{\mu}_{r+1})}{\sqrt{\sum_{k=1}^r \pi_k \sum_{k=1}^{r+1} \pi_k}}.$$

Therefore, the objective in (10) can be written as

$$\mathbb{E}(2^{-1}\|\mathbf{Y}' - \mathbf{X}'\mathbf{W}\|_F^2) = 2^{-1} \text{Tr}\{\mathbf{W}^\top \mathbf{G}\mathbf{W}\} - \text{Tr}\{\mathbf{W}^\top \tilde{\Delta}\} + o(1) + C. \quad (11)$$

Let $\mathbf{W}^* = \mathbf{G}^{-1}\tilde{\Delta}$, then \mathbf{W}^* is the minimizer of population loss function in (11) up to the $o(1)$ term. We further show that \mathbf{W}^* also corresponds to the matrix of discriminant vectors Θ_d up to orthogonal transformation and column-scaling.

Lemma 1. *Under factor model (4) and for $\alpha \in (0, 1]$, there exists orthogonal matrices \mathbf{R}_d such that $\mathbf{W}_d^* \mathbf{R}_d^\top$ is equal to Θ_d up to column scaling.*

Hence, the population loss (11) can be viewed as the quadratic loss with respect to discriminant vectors Θ_d with a particular choice of orthogonal transformation and scaling, which affect neither the classification rule nor the row-sparsity pattern. In what follows, we show that minimizer $\widehat{\mathbf{W}}$ of (9) is consistent at estimating \mathbf{W}^* under the following assumptions.

Assumption 1. Θ_d is row-sparse with the support $S_d = \{j : \|e_j^\top \Theta_d\|_2 \neq 0\}$ and $s_d = \text{card}(S_d)$. Hence \mathbf{W}_d^* is also row-sparse with the same support, and \mathbf{W}^* is row-sparse with the support $S = (S_1, \dots, S_D)$ and $s = \text{card}(S) = \sum_{d=1}^D s_d$.

Assumption 2. $P(y = k) = \pi_k$ for $k = 1, \dots, K$ with $0 < \pi_{\min} \leq \pi_k \leq \pi_{\max} < 1$.

Assumption 3. $\mathbf{x}_d|y = k \sim \mathcal{N}(\boldsymbol{\mu}_{dk}, \boldsymbol{\Sigma}_{dy})$ for all $k = 1, \dots, K$.

Assumption 4. Let $p_{max} = \max_d p_d$ and $p_{min} = \min_d p_d$. Then for some constant $C > 0$

$$\frac{\log(p_{max})}{\log(p_{min})} < C \text{ and } \log p_d = o(n), \text{ for all } d = 1, \dots, D.$$

These assumptions are typical for multivariate analysis methods and high-dimensional settings. Assumption 1 states that population matrices of discriminant vectors are row-sparse. Assumption 2 states that the class proportions are not degenerate. Assumption 3 states that the measurements are normally distributed conditionally on the class membership, it can be relaxed to sub-gaussianity without affecting the rates. Assumption 4 states that the views have comparable numbers of measurements for different views on the log scale, and allows to have larger number of measurements than the number of samples.

Similar to the assumptions required for estimation consistency in linear regression with group-lasso penalty (Nardi and Rinaldo, 2008; Lounici et al., 2011), we also require restricted eigenvalue condition satisfied on the weighted cone.

Definition 1 (Weighted cone). Let $\boldsymbol{\lambda} = (\lambda_1, \dots, \lambda_d)$ and $S = (S_1, \dots, S_D)$. Then

$$C(S, \boldsymbol{\lambda}) = \left\{ \mathbf{M} \in \mathbb{R}^{\sum_{d=1}^D p_d \times (K-1)} : \sum_{d=1}^D \lambda_d \|\mathbf{M}_{d, S_d^c}\|_{1,2} \leq 3 \sum_{d=1}^D \lambda_d \|\mathbf{M}_{d, S_d}\|_{1,2} \right\}.$$

Definition 2. A matrix $\mathbf{Q} \in \mathbb{R}^{q \times p}$ satisfies restricted eigenvalue condition $RE(S, \boldsymbol{\lambda})$ with parameter $\gamma_{\mathbf{Q}} = \gamma(S, \boldsymbol{\lambda}, \mathbf{Q})$ if for some set S , and for all $\mathbf{A} \in C(S, \boldsymbol{\lambda})$ it holds that

$$\|\mathbf{Q}\mathbf{A}\|_F^2 \geq \gamma_{\mathbf{Q}} \|\mathbf{A}\|_F^2.$$

We are now ready to state the main result. Let $\delta = \|\tilde{\boldsymbol{\Delta}}\|_{\infty, 2}$, let $g = \max_j \{\mathbf{G}^{-1}\}_{jj}$ be the largest diagonal entry of \mathbf{G}^{-1} , and let $\tau = \max_j \sqrt{\sigma_j^2 + \max_k \mu_{k,j}^2}$, where σ_j are diagonal elements of $\boldsymbol{\Sigma}_y$ and $\mu_{k,j}$ are elements of $\boldsymbol{\mu}_k$.

Theorem 2. Under Assumptions 1-4, if $\lambda_d = C(\tau \vee \tau^2 \delta g) D^{-1} \sqrt{(K-1) \log[(K-1)p_d]}/n$ for some constant $C > 0$, $s_d^2 \log[(K-1)p_d] = o(n)$ and $\mathbf{G}^{-1/2}$ satisfies condition $RE(S, \boldsymbol{\lambda})$ with parameter $\gamma = \gamma(S, \boldsymbol{\lambda}, \mathbf{G}^{-1/2})$, then

$$\|\widehat{\mathbf{W}} - \mathbf{W}^*\|_F = O_p \left((\tau \vee \tau^2 \delta g) \frac{1}{D\gamma} \sqrt{\frac{K-1}{n} \sum_{d=1}^D s_d \log[(K-1)p_d]} \right).$$

Remark 2. If $p_d \geq K$ for all d , then $\log[(K-1)p_d] = \log(K-1) + \log p_d < 2 \log p_d$, and the rate could be simplified to

$$\|\widehat{\mathbf{W}} - \mathbf{W}^*\|_F = O_p \left((\tau \vee \tau^2 \delta g) \frac{1}{D\gamma} \sqrt{\frac{K-1}{n} \sum_{d=1}^D s_d \log(p_d)} \right).$$

Our results allow both the number of variable p_d and the number of classes K to grow with n . The scaling requirement $s_d^2 \log[(K-1)p_d] = o(n)$ is needed to ensure that restricted eigenvalue condition on \mathbf{G} implies restricted eigenvalue condition on random $\mathbf{X}'^\top \mathbf{X}'$ via the infinity norm bound. When $K = 2$, $\widehat{\mathbf{W}}$ and \mathbf{W}^* are vectors, and this condition can be dropped using the results of Rudelson and Zhou (2013). Nevertheless, the estimation error itself has the same rate as estimation error in linear regression with group-lasso (Lounici et al., 2011; Nardi and Rinaldo, 2008). While our method can be viewed as multi-response linear regression due to formulation (9), the group lasso results cannot be directly applied for several reasons. First, both \mathbf{X}' and \mathbf{Y}' have dependencies across rows and contain fixed blocks of 0 values. Second, the linear model assumption between \mathbf{Y}' and \mathbf{X}' does not hold. Third, the residuals $\boldsymbol{\Psi} = \mathbf{Y}' - \mathbf{X}'\mathbf{W}^*$ do not have normal distribution and are dependent with \mathbf{X}' . These challenges required the use of different proof techniques, and the full proof of Theorem 2 can be found in Appendix A.

4 Implementation

4.1 Additional regularization via elastic net

It is well known that the lasso-type penalties can lead to erratic solution paths in the presence of highly-correlated variables (Hastie et al., 2015, Chapter 4.2). To overcome this drawback, Zou and Hastie (2005) propose an elastic net penalty which combines ridge and lasso penalties, thus making highly correlated variables either being jointly selected or not selected in the model. Zou and Hastie (2005) also advocate an extra scaling step which in regression context is equivalent to replacing the sample covariance matrix $\mathbf{X}'^\top \mathbf{X}'/n$ with the regularized version $(1-\rho)\mathbf{X}'^\top \mathbf{X}'/n + \rho\mathbf{I}$ for $\rho \in [0, 1]$. We adapt this idea to JACA, and replace $\mathbf{X}'^\top \mathbf{X}'$ in (9) with $(1-\rho)\mathbf{X}'^\top \mathbf{X}' + \rho\mathbf{I}$ for $\rho \in [0, 1]$ leading to

$$\underset{\mathbf{W}}{\text{minimize}} \left\{ \frac{1}{2} \|\mathbf{Y}' - \mathbf{X}'\mathbf{W}\|_F^2 - \frac{\rho}{2} \|\mathbf{X}'\mathbf{W}\|_F^2 + \frac{\rho}{2} \|\mathbf{W}\|_F^2 + \sum_{d=1}^D \lambda_d \text{Pen}(\mathbf{W}_d) \right\}. \quad (12)$$

Problem (12) is still convex, and the theoretical results of Section 3 can be extended to (12) (Hebiri and Van De Geer, 2011). When $\rho = 0$, problems (12) and (9) coincide.

4.2 Optimization algorithm

We use a block-coordinate descent algorithm to solve (12) for fixed values of $\rho \in [0, 1]$ and $\lambda_d \geq 0$. Let \mathbf{w}_{dj} be the j th row of \mathbf{W}_d , and let $\text{Pen}(\mathbf{W}_d) = \sum_{j=1}^{p_d} \|\mathbf{w}_{dj}\|_2$. Since (12) is convex, and the penalty is separable with respect to each \mathbf{w}_{dj} , the algorithm is guaranteed to converge to the global optimum from any starting point (Tseng, 2001).

We assume that each \mathbf{X}_d is standardized so that the diagonal entries of $n^{-1}\mathbf{X}_d^\top \mathbf{X}_d$ are equal to one. This standardization is common in the literature (Zou and Hastie, 2005; Witten and Tibshirani, 2009), and effectively results in penalizing each variable proportionally to

Algorithm 1 Block-coordinate descent algorithm for (12)

Given: $k = 0$, $\mathbf{W}^{(0)}$, $\varepsilon > 0$; $\mathbf{R} \leftarrow \mathbf{Y}' - (1 - \rho)\mathbf{X}'\mathbf{W}^{(0)}$;**while** $k \neq k_{max}$ and $\left| \text{objective}(\mathbf{W}^{(k)}) - \text{objective}(\mathbf{W}^{(k-1)}) \right| \geq \varepsilon$ **do** $k \leftarrow k + 1$; **for** $d = 1$ **to** D **do** **for** $j = 1$ **to** p_d **do** $\mathbf{w}_{dj}^{(k)} \leftarrow S_{\lambda_d}(\mathbf{X}'_{dj}\mathbf{R} + (1 - \rho)\|\mathbf{X}'_{dj}\|_2^2\mathbf{w}_{dj}^{(k-1)}) / \{(1 - \rho)\|\mathbf{X}'_{dj}\|_2^2 + \rho\}$; $\mathbf{R} \leftarrow \mathbf{R} + (1 - \rho)\mathbf{X}'_{dj}(\mathbf{w}_{dj}^{(k-1)} - \mathbf{w}_{dj}^{(k)})$ **end** **end****end**

its standard deviation. Moreover, using $\rho > 0$ with this standardization in (12) ensures the uniqueness of solution for any λ_d due to strict convexity of the objective function.

Consider solving (12) with respect to a row-vector \mathbf{w}_{dj} , and let \mathbf{X}'_{dj} be the corresponding column of \mathbf{X}' . The KKT conditions (Boyd and Vandenberghe, 2004) can be written as a set of $\sum_{d=1}^D p_d$ equations of the form

$$(1 - \rho)\mathbf{X}'_{dj}\mathbf{X}'\mathbf{W} + \rho\mathbf{w}_{dj} - \mathbf{X}'_{dj}\mathbf{Y}' + \lambda_d\mathbf{u}_{dj} = 0, \quad (13)$$

where \mathbf{u}_{dj} is the subgradient of $\|\mathbf{w}_{dj}\|_2$, that is $\mathbf{u}_{dj} = \mathbf{w}_{dj}/\|\mathbf{w}_{dj}\|_2$ when $\|\mathbf{w}_{dj}\|_2 \neq 0$ and $\mathbf{u}_{dj} \in \{\mathbf{u} : \|\mathbf{u}\|_2 \leq 1\}$ otherwise. Solving (13) with respect to \mathbf{w}_{dj} leads to

$$\mathbf{w}_{dj} = \{\mathbf{X}'_{dj}\mathbf{Y}' - (1 - \rho)\mathbf{X}'\mathbf{W} + (1 - \rho)\mathbf{X}'_{dj}\mathbf{w}_{dj} - \lambda_d\mathbf{u}_{dj}\} / \{(1 - \rho)\|\mathbf{X}'_{dj}\|_2^2 + \rho\}.$$

For a vector $\mathbf{v} \in \mathbb{R}^m$ and $\lambda > 0$, let $S_\lambda(\mathbf{v}) = \max(0, 1 - \lambda/\|\mathbf{v}\|_2)\mathbf{v}$ be the vector soft-thresholding operator. Then iterating block updates leads to Algorithm 1.

4.3 Selection of tuning parameters

JACA requires the specification of several parameters: $\alpha \in (0, 1]$ that controls the relative weights of LDA and CCA criteria, $\rho \in [0, 1]$ that controls the shrinkage induced by elastic net, and $\lambda_d \geq 0$ that control the sparsity level of each \mathbf{W}_d respectively. While it is possible to perform cross-validation over all of the parameters, due to computational considerations we restrict the space as follows. First, we set $\alpha = 0.5$ in all of our simulations studies and data analyses. Secondly, we set $\lambda_d = \epsilon\lambda_{\max,d}$ with $\epsilon \in (0, 1)$, where $\lambda_{\max,d}$ is such that $\widehat{\mathbf{W}}_d = \mathbf{0}$ for any $\lambda \geq \lambda_{\max,d}$, similar strategy is used in Luo et al. (2016) as it allows to control the sparsity of each \mathbf{W}_d at similar levels. The value of $\lambda_{\max,d}$ is given below.

Proposition 3. Let $\lambda_{\max,d} = \frac{\alpha}{nD}\|\mathbf{X}_d^\top\widetilde{\mathbf{Y}}\|_{\infty,2}$. Then $\mathbf{W}_d = \mathbf{0}$ for all $\lambda \geq \lambda_{\max,d}$.

We use cross-validation with F folds to select $\rho \in [0, 1]$ and $\epsilon \in [10^{-4}, 1]$, with a course grid for ρ and a fine grid for ϵ .

It is typical to minimize the prediction error in cross-validation, for example the least squares error in the linear regression. In our context, however, both classification rules and correlation measures are invariant to the scale of \mathbf{W}_d , hence we need a scale-invariant metric. We propose to consider

$$CV(\rho, \epsilon) = \frac{1}{F} \sum_{f=1}^F \left\{ \alpha \sum_{d=1}^D |\text{Cor}(\tilde{\mathbf{Y}}^{(f)}, \mathbf{X}_d^{(f)} \widehat{\mathbf{W}}_d^{(-f)})| + \frac{(1-\alpha)}{D-1} \sum_{d=1}^{D-1} \sum_{l=d+1}^D |\text{Cor}(\mathbf{X}_d^{(f)} \mathbf{W}_d^{(-f)}, \mathbf{X}_l^{(f)} \mathbf{W}_l^{(-f)})| \right\}, \quad (14)$$

where $\tilde{\mathbf{Y}}^{(f)}$, $\mathbf{X}_d^{(f)}$ correspond to the samples in the f th fold; and $\widehat{\mathbf{W}}_d^{(-f)}$ are solutions to (12) with given ρ and ϵ based on samples in all folds except the f th. We define the correlation between two centered matrices \mathbf{X} and \mathbf{Y} as the square root of the RV-coefficient (Robert and Escoufier, 1976), where

$$\text{RV}(\mathbf{X}, \mathbf{Y}) := \frac{\text{Tr}(\mathbf{X}\mathbf{X}^\top \mathbf{Y}\mathbf{Y}^\top)}{\sqrt{\text{Tr}(\mathbf{X}\mathbf{X}^\top)^2} \sqrt{\text{Tr}(\mathbf{Y}\mathbf{Y}^\top)^2}}.$$

By definition, $\sqrt{\text{RV}(\mathbf{X}, \mathbf{Y})} \in [0, 1]$, and is invariant to scale and orthogonal transformation. If \mathbf{X} and \mathbf{Y} are vectors, then $\sqrt{\text{RV}(\mathbf{X}, \mathbf{Y})} = |\text{Cor}(\mathbf{X}, \mathbf{Y})|$.

5 Missing data case - semi-supervised learning

In the joint analysis of multi-view data, it is typical to perform complete case analysis, that is only consider the subjects for which all the views are available. This is often not the case in practice. One example is described in Section 7, where out of 282 subjects with RNAseq data, only 218 have also available miRNA measurements. Moreover, 51 subjects out of these 218 have no class labels, and therefore can not be used to train supervised classification algorithms. Most of the available methods require either imputation of missing views/group labels, or perform complete case analysis (only use samples for which all the views and the group labels are available). A particular advantage of our framework is that we can also use the samples for which we have either a class-label or at least two views available without the need to impute the missing values. In other words, our proposal allows to perform semi-supervised learning, that is to use information from both labeled and unlabeled subjects to construct classification rules. In what follows, we assume that for each view and each subject, the measurements are rather completely missing, or not missing at all, that is we do not consider the case where a subset of measurements from one view is missing.

Consider an equivalent representation of (8) as

$$\begin{aligned} \text{minimize}_{\mathbf{W}_1, \dots, \mathbf{W}_D} \left\{ \frac{\alpha}{2nD} \sum_{d=1}^D \sum_{i=1}^n \|\tilde{\mathbf{y}}_i - \mathbf{x}_{id}^\top \mathbf{W}_d\|_2^2 \right. \\ \left. + \frac{\alpha}{2nD(D-1)} \sum_{d=1}^D \sum_{l=d+1}^D \sum_{i=1}^n \|\mathbf{x}_{id}^\top \mathbf{W}_d - \mathbf{x}_{il}^\top \mathbf{W}_l\|_2^2 + \sum_{d=1}^D \lambda_d \text{Pen}(\mathbf{W}_d) \right\}, \end{aligned} \quad (15)$$

where \mathbf{x}_{id} is the i th row of matrix \mathbf{X}_d . Next, assume some samples have missing views or class labels. Let A_{dy} be the subset of samples (out of n) for which both class label and view d are available, and let B_{dl} be the subset of samples for which both views d and l are available. In case there are no missing labels/views, $A_{dy} = B_{dl} = \{1, \dots, n\}$ for all $d = 1, \dots, D$, $l = 1, \dots, D$. Then (15) can be rewritten as

$$\begin{aligned} \text{minimize}_{\mathbf{W}_1, \dots, \mathbf{W}_D} \left\{ \frac{\alpha}{2nD} \sum_{d=1}^D \sum_{i \in A_{dy}} \|\tilde{\mathbf{y}}_i - \mathbf{x}_{id}^\top \mathbf{W}_d\|_2^2 \right. \\ \left. + \frac{\alpha}{2nD(D-1)} \sum_{d=1}^{D-1} \sum_{l=d+1}^D \sum_{i \in B_{dl}} \|\mathbf{x}_{id}^\top \mathbf{W}_d - \mathbf{x}_{il}^\top \mathbf{W}_l\|_2^2 + \sum_{d=1}^D \lambda_d \text{Pen}(\mathbf{W}_d) \right\}, \end{aligned} \quad (16)$$

that is we can use all samples with class labels and at least one view for the first part (discriminant analysis), and all samples with at least two views for the second part (canonical correlation analysis). The only samples that we can not use are the ones for which there is no class label and only one view. Like (15), problem (16) is convex, and can be rewritten as multi-response linear regression problem using augmented data approach similar to Section 2.3. This means that the implementation of Section 4 can also be used for problem (16). We refer to (16) as semi-supervised JACA (ssJACA).

6 Simulation studies

We compare the performance of the following methods: (i) JACA: Joint Association and Classification Analysis, the proposed approach; (ii) Sparse Linear Discriminant Analysis of Gaynanova et al. (2016) as implemented in the R package MGSDA (Gaynanova, 2016), either applied separately to each dataset (SLDA_sep), or jointly on concatenated dataset (SLDA_joint); (iii) Sparse CCA: Sparse Canonical Correlation Analysis of Witten and Tibshirani (2009) as implemented in the R package PMA (Witten et al., 2013). We use cross-validation to choose the tuning parameters instead of the permutation method introduced in Witten and Tibshirani (2009), since the former one gives better results. (iv) Sparse sCCA: Sparse supervised CCA proposed in Witten and Tibshirani (2009). We first choose a set of variables with largest values of F-statistic from a one-way ANOVA, and then apply Sparse CCA with selected variables; (v) CVR: Canonical Variate Regression by Luo et al. (2016) as implemented in the corresponding R package (Luo and Chen, 2017).

6.1 Data generation

We generate the data using factor model (4). Specifically, given $\tilde{\Sigma}_d$, $d = 1, \dots, D$, we generate the factor loadings in (4) as follows

1. Generate row-sparse matrix $\mathbf{B}_d \in \mathbb{R}^{p_d \times K-1}$ with $s = 10$ non-zero rows. Draw nonzero elements from uniform distribution on $[-2, -1] \cup [1, 2]$. Given $c_d > 0$, rotate and scale \mathbf{B}_d so that $\mathbf{B}_d^\top \tilde{\Sigma}_d \mathbf{B}_d = \text{diag}(c_d^2)$, and set $\Delta_d = \tilde{\Sigma}_d \mathbf{B}_d$. According to Theorem 1, this sets $K - 1$ canonical correlations ρ_k between datasets d and l to be equal to $\rho_k = (c_d c_l) / \sqrt{(1 + c_d^2)(1 + c_l^2)}$.
2. If $q \neq 0$, generate $\mathbf{M}_d \in \mathbb{R}^{p_d \times q}$ with elements from $N(0, 1)$, orthogonalize \mathbf{M}_d with respect to Δ_d as $\mathbf{M}_d = (\mathbf{I} - \mathbf{P}_{\Delta_d}) \mathbf{M}_d$, where \mathbf{P}_{Δ_d} is the projection matrix onto column space of Δ_d . For canonical correlation $\rho_k \in (0, 1)$, set $c_k = \sqrt{\rho_k / (1 - \rho_k)}$, and rotate and scale \mathbf{M}_d so that $\mathbf{M}_d^\top \tilde{\Sigma}_d \mathbf{M}_d = \text{diag}(c_k^2)$. Set $\mathbf{A}_d = \tilde{\Sigma}_d \mathbf{M}_d$.

We further draw n independent y with $P(y = k) = \pi_k$, n independent \mathbf{u}_q from $N(0, \mathbf{I}_q)$, and n independent $\mathbf{e}_1, \dots, \mathbf{e}_d$, each from $N(0, \mathbf{I}_{p_d})$. We get n replicas $\mathbf{X}_1, \dots, \mathbf{X}_d$ according to (4) with given Δ_d , \mathbf{A}_d and $\boldsymbol{\mu}_d = 0$, $d = 1, \dots, D$. By construction, the population discriminant vectors are proportional to \mathbf{B}_d with corresponding row-sparsity pattern.

6.2 Evaluation criteria

We compare the methods in terms of estimation consistency and strength of association between the views, the variable selection comparison is provided in Appendix D. Let $\Theta_d \propto \tilde{\Sigma}_d^{-1} \Delta_d \in \mathbb{R}^{p_d \times (K-1)}$ be the population matrix of class-specific canonical vectors for view d with $\tilde{\Sigma}_d$ as in (4), and \mathbf{W}_d be the estimated matrix. To evaluate estimation performance, we consider

$$\text{Cor}_\Sigma(\mathbf{W}_d, \Theta_d) = \left(\frac{\text{Tr}(\mathbf{W}_d^\top \tilde{\Sigma}_d \Theta_d \Theta_d^\top \tilde{\Sigma}_d \mathbf{W}_d)}{\sqrt{\text{Tr}(\mathbf{W}_d^\top \tilde{\Sigma}_d \mathbf{W}_d)^2} \sqrt{\text{Tr}(\Theta_d^\top \tilde{\Sigma}_d \Theta_d)^2}} \right)^{\frac{1}{2}}$$

as a measure of similarity between \mathbf{W}_d and Θ_d with $\text{Cor}_\Sigma(\mathbf{W}_d, \Theta_d) = 1$ if and only if \mathbf{W}_d is equal to Θ_d up to scaling and orthogonal transformation, and $\text{Cor}_\Sigma(\mathbf{W}_d, \Theta_d) = 0$ if $\mathbf{W}_d^\top \tilde{\Sigma}_d \Theta_d = 0$.

To evaluate the strength of found association between the views, we consider

$$\text{Sum correlation}(\mathbf{W}_1, \dots, \mathbf{W}_D) = \sum_{d=1}^{D-1} \sum_{l=d+1}^D \text{Cor}_\Sigma(\mathbf{W}_d, \mathbf{W}_l),$$

where

$$\text{Cor}_\Sigma(\mathbf{W}_d, \mathbf{W}_l) = \left(\frac{\text{Tr}(\mathbf{W}_d^\top \Sigma_{dl} \mathbf{W}_l \mathbf{W}_l^\top \Sigma_{dl} \mathbf{W}_d)}{\sqrt{\text{Tr}(\mathbf{W}_d^\top \Sigma_d \mathbf{W}_d)^2} \sqrt{\text{Tr}(\mathbf{W}_l^\top \Sigma_l \mathbf{W}_l)^2}} \right)^{\frac{1}{2}},$$

(p_1, p_2)	Cor_Σ	JACA	SLDA sep	SLDA joint	Sparse CCA	Sparse sCCA	CVR
(100,100)	(\mathbf{W}_1, Θ_1)	0.839 (0.002)	0.823 (0.003)	0.835 (0.002)	0.752 (0.002)	0.740 (0.002)	0.756 (0.007)
	(\mathbf{W}_2, Θ_2)	0.907 (0.003)	0.889 (0.005)	0.825 (0.006)	0.841 (0.003)	0.825 (0.003)	0.704 (0.013)
	$(\mathbf{W}_1, \mathbf{W}_2)$	0.752 (0.001)	0.744 (0.001)	0.732 (0.002)	0.715 (0.001)	0.708 (0.001)	0.670 (0.006)
(100,500)	(\mathbf{W}_1, Θ_1)	0.842 (0.002)	0.824 (0.003)	0.833 (0.002)	0.755 (0.002)	0.742 (0.001)	0.751 (0.007)
	(\mathbf{W}_2, Θ_2)	0.893 (0.003)	0.882 (0.003)	0.816 (0.005)	0.844 (0.003)	0.734 (0.003)	0.666 (0.011)
	$(\mathbf{W}_1, \mathbf{W}_2)$	0.750 (0.001)	0.743 (0.001)	0.730 (0.001)	0.717 (0.001)	0.685 (0.001)	0.656 (0.006)
(500,500)	(\mathbf{W}_1, Θ_1)	0.839 (0.002)	0.839 (0.002)	0.830 (0.002)	0.758 (0.001)	0.711 (0.002)	0.745 (0.006)
	(\mathbf{W}_2, Θ_2)	0.897 (0.003)	0.883 (0.003)	0.817 (0.006)	0.836 (0.003)	0.738 (0.003)	0.674 (0.009)
	$(\mathbf{W}_1, \mathbf{W}_2)$	0.750 (0.001)	0.747 (0.001)	0.729 (0.002)	0.716 (0.001)	0.677 (0.001)	0.661 (0.005)

Table 1: Comparison of estimation correlation of Case 1 over 100 replications when $D = 2$, $K = 2$, and $\tilde{\Sigma}_{dy}$ follows auto-correlation structure. Standard errors are given in the brackets and the highest values are highlighted in bold.

Σ_d is the marginal covariance matrix of view d , and Σ_{dl} is the marginal cross-covariance matrix of view d and l as in Section 2.2. This criterion is similar to sum correlation in Gross and Tibshirani (2015), however our definition uses population covariance matrices rather than the sample counterparts.

6.3 Two datasets, two groups

We set $n = 160$, $K = 2$, and generate n independent $y \in \{1, 2\}$ with $\pi_1 = 0.4$, and pairs $(\mathbf{x}_1, \mathbf{x}_2) \in \mathbb{R}^{p_1} \times \mathbb{R}^{p_2}$ with $(p_1, p_2) \in \{(100, 100), (100, 500), (500, 500)\}$ following Section 6.1. We consider autocorrelation structures $\tilde{\Sigma}_1 = (0.8^{|i-j|})_{ij}$, $\tilde{\Sigma}_2 = (0.5^{|i-j|})_{ij}$, and set the value of canonical correlation due to shared class as $\rho = 0.8$ by letting $c_1 = c_2 = \sqrt{\rho/(1-\rho)}$ in generating B_d in Section 6.1. We consider the following cases for other shared factors:

Case 1: $q = 0$, no shared factors except class y ;

Case 2: $q = 2$ with corresponding values for canonical correlations being 0.6 and 0.5;

Case 3: $q = 2$ with corresponding values for canonical correlations being 0.9 and 0.5.

In Case 2, the leading canonical correlation between the views is due to shared class membership despite the presence of other shared factors, whereas in Case 3 the leading canonical correlation is due to factors independent from class membership. We consider 100 replications for each case. The results are summarized in Tables 1–3.

JACA gives the best estimation results in most scenarios, and has low estimation variance. JACA also performs the best in terms of sum correlation except for Case 3, where sum correlation for Sparse CCA is stronger. This is not surprising, since in Case 3 the largest canonical correlation is due to the factor independent from class membership. Thus, the loadings estimated from sparse CCA are almost orthogonal to the true discriminant vectors

(p_1, p_2)	Cor_Σ	JACA	SLDA sep	SLDA joint	Sparse CCA	Sparse sCCA	CVR
(100,100)	(\mathbf{W}_1, Θ_1)	0.840 (0.002)	0.825 (0.003)	0.836 (0.002)	0.687 (0.016)	0.744 (0.002)	0.726 (0.010)
	(\mathbf{W}_2, Θ_2)	0.907 (0.003)	0.883 (0.006)	0.816 (0.006)	0.755 (0.020)	0.823 (0.003)	0.697 (0.011)
	$(\mathbf{W}_1, \mathbf{W}_2)$	0.752 (0.001)	0.742 (0.002)	0.728 (0.002)	0.686 (0.006)	0.704 (0.001)	0.641 (0.009)
(100,500)	(\mathbf{W}_1, Θ_1)	0.844 (0.001)	0.825 (0.003)	0.834 (0.002)	0.704 (0.017)	0.745 (0.002)	0.718 (0.010)
	(\mathbf{W}_2, Θ_2)	0.895 (0.003)	0.883 (0.002)	0.818 (0.004)	0.780 (0.021)	0.732 (0.003)	0.640 (0.010)
	$(\mathbf{W}_1, \mathbf{W}_2)$	0.751 (0.001)	0.743 (0.001)	0.731 (0.001)	0.681 (0.011)	0.682 (0.001)	0.623 (0.008)
(500,500)	(\mathbf{W}_1, Θ_1)	0.838 (0.002)	0.840 (0.002)	0.831 (0.002)	0.592 (0.029)	0.711 (0.002)	0.718 (0.007)
	(\mathbf{W}_2, Θ_2)	0.898 (0.003)	0.884 (0.003)	0.817 (0.006)	0.657 (0.033)	0.738 (0.003)	0.637 (0.011)
	$(\mathbf{W}_1, \mathbf{W}_2)$	0.750 (0.001)	0.748 (0.001)	0.729 (0.002)	0.604 (0.021)	0.676 (0.001)	0.632 (0.006)

Table 2: Comparison of estimation correlation of Case 2 over 100 replications when $D = 2$, $K = 2$, and $\tilde{\Sigma}_{dy}$ follows auto-correlation structure. Standard errors are given in the brackets and the highest values are highlighted in bold.

(p_1, p_2)	Cor_Σ	JACA	SLDA sep	SLDA joint	Sparse CCA	Sparse sCCA	CVR
(100,100)	(\mathbf{W}_1, Θ_1)	0.843 (0.001)	0.830 (0.003)	0.837 (0.002)	0.098 (0.004)	0.682 (0.015)	0.727 (0.007)
	(\mathbf{W}_2, Θ_2)	0.904 (0.003)	0.888 (0.005)	0.805 (0.006)	0.040 (0.003)	0.720 (0.017)	0.714 (0.009)
	$(\mathbf{W}_1, \mathbf{W}_2)$	0.751 (0.001)	0.744 (0.002)	0.724 (0.002)	0.874 (0.000)	0.715 (0.003)	0.549 (0.017)
(100,500)	(\mathbf{W}_1, Θ_1)	0.844 (0.002)	0.822 (0.004)	0.833 (0.002)	0.117 (0.004)	0.728 (0.007)	0.731 (0.006)
	(\mathbf{W}_2, Θ_2)	0.896 (0.003)	0.884 (0.002)	0.820 (0.005)	0.043 (0.003)	0.700 (0.007)	0.625 (0.010)
	$(\mathbf{W}_1, \mathbf{W}_2)$	0.751 (0.001)	0.742 (0.001)	0.731 (0.001)	0.861 (0.000)	0.684 (0.002)	0.553 (0.014)
(500,500)	(\mathbf{W}_1, Θ_1)	0.839 (0.002)	0.842 (0.001)	0.831 (0.002)	0.033 (0.002)	0.694 (0.004)	0.714 (0.008)
	(\mathbf{W}_2, Θ_2)	0.898 (0.003)	0.885 (0.003)	0.817 (0.006)	0.033 (0.003)	0.716 (0.005)	0.636 (0.009)
	$(\mathbf{W}_1, \mathbf{W}_2)$	0.750 (0.001)	0.748 (0.001)	0.729 (0.002)	0.854 (0.000)	0.675 (0.001)	0.573 (0.012)

Table 3: Comparison of estimation correlation of Case 3 over 100 replications when $D = 2$, $K = 2$, and $\tilde{\Sigma}_{dy}$ follows auto-correlation structure. Standard errors are given in the brackets and the highest values are highlighted in bold.

Θ_d as demonstrated by low values of $\text{Cor}_\Sigma(\mathbf{W}_d, \Theta_d)$. Finally, CVR is better than Sparse CCA in Cases 2 and 3 in terms of estimation performance, however, it performs worse than JACA and SLDA methods. We conjecture this is likely due to CVR using logistic model for estimation rather than factor model (4).

Next, we evaluate the performance of semi-supervised JACA (ssJACA) described in Section 5. We generate $n = 200$ samples as before, and set class information for 100 samples as missing, so that $n_1 = 100$ samples have complete view and class information, whereas the remaining $n_2 = 100$ samples have information on both views but no class assignment. We compare JACA based on $n_1 = 100$ complete samples with ssJACA based on all $n_1 + n_2 = 200$ samples. The results over 100 replications are displayed in Figure 1. In every scenario, ssJACA improves JACA in both estimation consistency and sum correlation, confirming the advantage of incorporating samples with missing class information in the analysis.

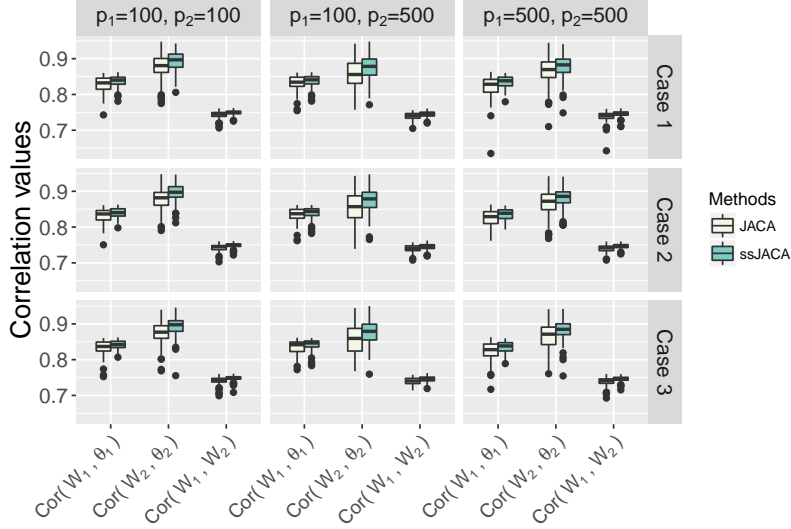


Figure 1: Comparison between JACA and semi-supervised JACA (ssJACA) over 100 replications when $D = 2$, $K = 2$. JACA uses 100 samples with complete view/class information, whereas ssJACA additionally uses 100 samples with missing class information.

6.4 Multiple datasets, multiple groups

We set $n = 240$, $K = 3$, and generate n independent $y \in \{1, 2, 3\}$ with $\pi_1 = 0.4$, $\pi_2 = \pi_3 = 0.3$. We also generate n tuples $(\mathbf{x}_1, \mathbf{x}_2, \mathbf{x}_3) \in \mathbb{R}^{p_1} \times \mathbb{R}^{p_2} \times \mathbb{R}^{p_3}$ with $p_1 = p_2 = p_3 \in \{100, 500\}$ following Section 6.1, and set $\tilde{\Sigma}_1 = (0.8^{|i-j|})_{ij}$, $\tilde{\Sigma}_2 = (0.5^{|i-j|})_{ij}$ and $\tilde{\Sigma}_3 = \mathbf{I}$. We let canonical correlations due to class membership be $\rho_1 = \rho_2 = 0.8$, and consider the following cases for other shared factors:

Case 1: $q = 0$, no shared factors except class y ;

Case 2: $q = 3$ with $\rho_3 = \rho_4 = \rho_5 = 0.6$;

Case 3: $q = 3$ with $\rho_3 = 0.9$, $\rho_4 = 0.9$, $\rho_5 = 0.5$.

We do not consider Sparse CCA methods because they are not directly applicable to the case of more than two views and more than two classes. While the issue of more than two views can be addressed by Multi CCA generalization (Witten and Tibshirani, 2009), both Sparse CCA and Multi CCA find $K - 1$ pairs of canonical vectors sequentially. As a result, one also needs to tune sparsity parameters sequentially leading to computationally expensive procedure with different sparsity patterns across canonical vector pairs. We also do not consider CVR as it is only implemented for binary classification problem.

The results for JACA and SLDA methods are reported in Table 4. JACA performs the best in terms of estimation consistency in most scenarios, and always performs the best in terms of sum correlation. When $p = 100$, JACA has similar performance with SLDA_sep,

		$p_1 = p_2 = p_3 = 100$			$p_1 = p_2 = p_3 = 500$		
	Cor_{Σ}	JACA	SLDA sep	SLDA joint	JACA	SLDA sep	SLDA joint
Case 1	(\mathbf{W}_1, Θ_1)	0.903 (0.002)	0.906 (0.002)	0.795 (0.002)	0.848 (0.002)	0.825 (0.003)	0.800 (0.002)
	(\mathbf{W}_2, Θ_2)	0.945 (0.001)	0.929 (0.003)	0.794 (0.008)	0.937 (0.001)	0.913 (0.004)	0.801 (0.008)
	(\mathbf{W}_3, Θ_3)	0.959 (0.001)	0.960 (0.002)	0.710 (0.010)	0.969 (0.001)	0.961 (0.003)	0.726 (0.011)
	Sum Correlation	2.321 (0.001)	2.309 (0.004)	1.196 (0.021)	2.282 (0.001)	2.185 (0.011)	1.231 (0.023)
Case 2	(\mathbf{W}_1, Θ_1)	0.908 (0.002)	0.914 (0.002)	0.795 (0.002)	0.850 (0.002)	0.827 (0.003)	0.798 (0.002)
	(\mathbf{W}_2, Θ_2)	0.946 (0.001)	0.931 (0.003)	0.799 (0.007)	0.937 (0.001)	0.921 (0.003)	0.797 (0.007)
	(\mathbf{W}_3, Θ_3)	0.959 (0.001)	0.962 (0.002)	0.709 (0.010)	0.969 (0.001)	0.963 (0.002)	0.726 (0.010)
	Sum Correlation	2.322 (0.001)	2.314 (0.002)	1.190 (0.020)	2.282 (0.001)	2.186 (0.010)	1.213 (0.023)
Case 3	(\mathbf{W}_1, Θ_1)	0.917 (0.002)	0.921 (0.002)	0.802 (0.002)	0.855 (0.002)	0.828 (0.003)	0.799 (0.002)
	(\mathbf{W}_2, Θ_2)	0.948 (0.001)	0.930 (0.003)	0.805 (0.007)	0.937 (0.001)	0.914 (0.004)	0.794 (0.008)
	(\mathbf{W}_3, Θ_3)	0.957 (0.001)	0.963 (0.002)	0.702 (0.010)	0.967 (0.001)	0.960 (0.003)	0.719 (0.010)
	Sum Correlation	2.326 (0.001)	2.316 (0.003)	1.196 (0.020)	2.284 (0.002)	2.183 (0.011)	1.206 (0.022)

Table 4: Comparison of estimation correlation over 100 replication when $D = 3$, $K = 3$. Standard errors are given in the brackets and the highest values are highlighted in bold.

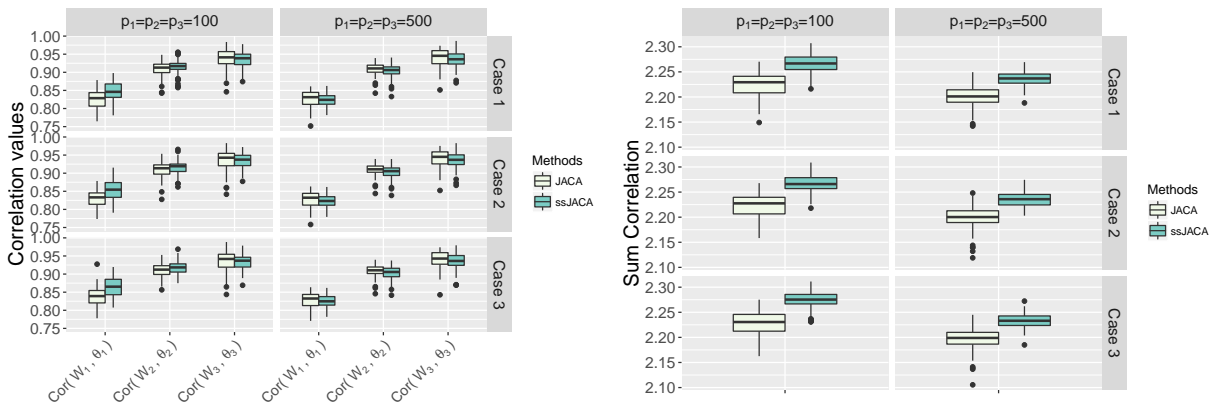


Figure 2: Comparison between JACA and semi-supervised JACA (ssJACA) over 100 replications when $D = 3$, $K = 3$. JACA uses 100 samples with complete view/class information, whereas ssJACA additionally uses 100 samples with missing class information.

but SLDA_sep’s performance decreases significantly as p increases. On the other hand, SLDA_joint performs poorly in most cases.

Next, we evaluate the performance of semi-supervised JACA (ssJACA) described in Section 5. Similar to Section 6.3, we generate $n = 200$ samples with $D = 3$, $K = 3$, and set class information for 100 samples as missing. We compare JACA based on $n_1 = 100$ complete samples with ssJACA based on all $n_1 + n_2 = 200$ samples. The results over 100 replications are displayed in Figure 2. When $p_1 = p_2 = p_3 = 100$, ssJACA improves JACA in both estimation performance and in sum correlation. When $p_1 = p_2 = p_3 = 500$, the performance of the two methods is similar in estimation, but ssJACA obtains higher sum correlation confirming the advantage of incorporating samples with missing class information.

CMS class	RNAseq	miRNA	Sample size
yes	yes	yes	167
yes	yes	no	27
no	yes	yes	51
no	yes	no	37
			Total: 282

Table 5: Number of available samples in COAD data with different missing patterns of CMS class/RNAseq/miRNA. Complete cases analysis will only be able to use 167 samples, whereas our semi-supervised approach allows to use 245 (all except the last row).

7 Data analysis

We consider the colorectal cancer (COAD) data from The Cancer Genome Atlas project with two views: RNAseq data of normalized counts and miRNA expression. We also analyzed breast cancer data from The Cancer Genome Atlas project, the results of that analysis can be found in Appendix E.2. We extracted samples corresponding to primary tumor tissue using TCGA2STAT R package (Wan et al., 2015). To account for data skewness and zero counts, we further log10-transformed both datasets with offset 1, and filtered the data to select 1572 variables for RNA-Seq and 375 for miRNA with highest standard deviation across samples. Recently, the Colorectal Cancer Consortium determined 4 consensus molecular subtypes (CMS) of colorectal cancer based on gene expression (Guinney et al., 2015), and we have extracted the assigned subtypes for COAD data from the Synapse platform (Synapse ID syn2623706). The resulting data has 282 subjects in total, with Table 5 displaying the pattern of available information for each subject. Our primary goal is to identify covarying patterns between RNA-Seq and miRNA data that are relevant for subtype discrimination.

First, we compare different methods from Section 6 using the subset of subjects with complete views and subtype information ($n = 167$). We do not consider CVR since it is only implemented for the binary classification problem. We randomly select 137 subjects for training and 35 for testing for the total of 100 random splits. The average misclassification error rates and the number of selected variables for each method are presented in Table 6. We consider two prediction approaches for each method: prediction based on one view alone (either RNA-seq or miRNA) using the corresponding subset of canonical vectors, and prediction using the concatenated dataset. In general, the performance using miRNA data is worse, which is not surprising since the subtypes were determined using gene expression data alone (Guinney et al., 2015). Although JACA selects more variables than SLDA_sep, it performs the best in terms of misclassification error rates, with SLDA_sep being the second best. SLDA_joint achieves a competitive misclassification rate using RNAseq data but not miRNA. We conjecture this is because RNAseq view has a much stronger class-specific signal that masks miRNA’s signal when datasets are concatenated. This explanation is supported by the mean number of variables selected by SLDA_joint from each view. Both supervised

Method	Misclassification Rate (%)			Cardinality		
	RNAseq	miRNA	Both	RNAseq	miRNA	Both
JACA	2.06 (0.30)	6.03 (0.49)	3.49 (0.35)	385.1 (8.8)	202.3 (3.4)	587.4 (12.2)
SLDA_sep	3.91 (0.42)	7.97 (0.61)	4.03 (0.41)	65.4 (3.1)	57.8 (1.6)	123.2 (3.7)
SLDA_joint	4.26 (0.45)	53.26 (1.82)	4.11 (0.46)	59.5 (2.8)	3.3 (0.4)	62.8 (3.2)
Sparse sCCA	41.89 (0.34)	47.71 (0.47)	42.6 (0.30)	932.5 (4.0)	251.4 (1.0)	1183.9 (4.6)
Sparse CCA	42.11 (0.35)	47.97 (0.46)	42.37 (0.34)	1287.5 (6.9)	369.5 (0.6)	1657 (6.8)

Table 6: Mean misclassification error rates in percentages and mean number of selected features over 100 random splits of 167 samples from COAD data with complete information, standard errors are given in brackets and the lowest values are highlighted in bold.

	JACA	SLDA_sep	SLDA_joint
Correlation	0.95 (0.002)	0.88 (0.003)	0.36 (0.027)

Table 7: Analysis based on 167 samples from COAD data with complete view and subtype information based on 100 random splits. Mean correlation between $\mathbf{X}_1 \widehat{\mathbf{W}}_1$ and $\mathbf{X}_2 \widehat{\mathbf{W}}_2$ where $\mathbf{X}_1, \mathbf{X}_2$ are samples from test data, and $\widehat{\mathbf{W}}_1, \widehat{\mathbf{W}}_2$ are estimated from the training data, standard errors are given in brackets and the highest value is highlighted in bold.

and unsupervised CCA methods perform poorly in classification. Based on results from Section 6, this suggests that the subtype-specific association between the views is weak compared to association due to other common factors.

We also compare the out-of-sample correlation values, that is $\text{Cor}(\mathbf{X}_1 \widehat{\mathbf{W}}_1, \mathbf{X}_2 \widehat{\mathbf{W}}_2)$, where $(\mathbf{X}_1, \mathbf{X}_2)$ are RNAseq and miRNA data from test samples, and $\widehat{\mathbf{W}}_1, \widehat{\mathbf{W}}_2$ are estimated on the training data. We do not consider CCA methods due to their poor classification performance. The results are presented in Table 7, with JACA achieving the strongest correlation value.

We further compare JACA fitted on 167 subjects (all views and subtypes available) with semi-supervised JACA fitted on 245 subjects (at least two views available). Both methods achieve the same misclassification rates on 167 subjects. For 27 subjects with missing miRNA data, the subtypes can only be predicted based on RNAseq. JACA has 11.11% misclassification rate on these 27 subjects, whereas ssJACA has 0% misclassification rate. This is perhaps not surprising since these 27 subjects are used by ssJACA for training, however it does show that including additional subjects changes the resulting classification rule. Similarly, for 51 subjects with missing subtype information, the correlation between $\mathbf{X}_1^* \widehat{\mathbf{W}}_1$ and $\mathbf{X}_2^* \widehat{\mathbf{W}}_2$ for JACA and ssJACA methods are 0.84 and 0.92 respectively, demonstrating that ssJACA leads to higher associations between the views. Table 8 shows the numbers of features selected by both methods. We observe that there is a significant overlap in the selected features, with ssJACA selecting a larger number.

The heatmaps of RNAseq and miRNA data with features selected by ssJACA are shown

	JACA	ssJACA	Intersection
RNA-seq	277	345	227
miRNA	164	188	161

Table 8: Numbers of features selected by JACA and ssJACA on COAD data. JACA is trained using 167 subjects and ssJACA is trained using 245 subjects. The last column corresponds to the number of features shared by both approaches.

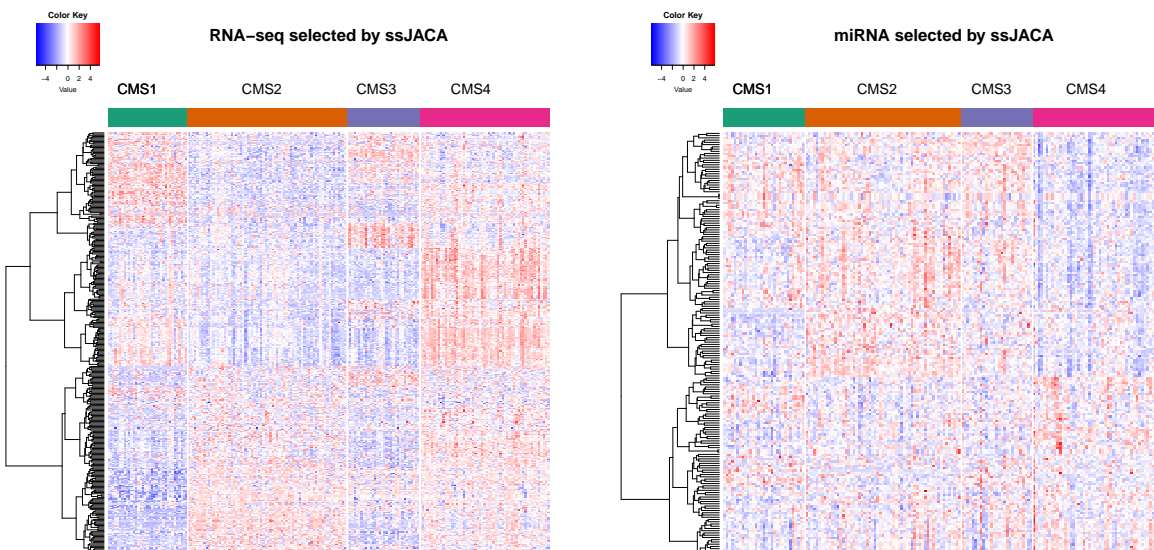


Figure 3: Heatmaps of RNaseq and miRNA views from COAD data based on features selected by ssJACA. We use Ward’s linkage with euclidean distances for feature ordering.

in Figure 3, an enlarged version of this Figure as well as a projection of data onto the space spanned by the canonical vectors can be found in Appendix E.1. Both views demonstrate different patterns across CMS classes, with the separation on RNaseq being visually much clearer. This is not surprising as CMS classes have been determined based on gene expression data only. Our analysis, however, also allows to determine co-varying patterns in miRNA, with subtype CMS4 being visually the most distinct in that view.

8 Discussion

In this work, we develop a joint framework for classification and association analysis of multi-view data by exploring the connections between linear discriminant analysis and canonical correlation analysis. A particular advantage of our approach is that it allows to use both samples with missing class labels and samples with missing subset of views. Nevertheless,

there are several parts of the method that requires further investigation. First, the trade off between classification and association criteria in (8) is controlled by the parameter α . While we fix $\alpha = 1/2$ for the analysis, it would be of interest to investigate whether there is an optimal value, both from empirical and theoretical perspectives. Secondly, we treat all views equally within our framework, however in practice some views may have stronger associations with class membership as well as with each other. This scenario can be addressed by adding view-specific weights within (8), however it is unclear how to choose the weights in practice. Finally, we focused on row-sparse structure via group-lasso penalty, however the method could be used with other structured penalties depending on the problem of interest.

Acknowledgements

This work was supported by NSF DMS-1712943.

A Proofs of the main results in the paper

Proof of Proposition 1

Proof. Under the stated conditions, \mathbf{x}_d in (3) satisfies (2) by construction, therefore it remains to show the reverse. Consider (2) with $\Sigma_{ldy} = \mathbf{0}$. Then

$$\mathbf{x}_d = \boldsymbol{\mu}_d + \sum_{k=1}^K (\boldsymbol{\mu}_{dk} - \boldsymbol{\mu}_d) \mathbb{1}\{y = k\} + \Sigma_{dy}^{1/2} \mathbf{e}_d,$$

where \mathbf{e}_d are independent from y . We next show that there exists function $f : \{1, 2, \dots, K\} \rightarrow \mathbb{R}^{K-1}$ such that $\boldsymbol{\mu}_d + \sum_{k=1}^K (\boldsymbol{\mu}_{dk} - \boldsymbol{\mu}_d) \mathbb{1}\{y = k\} = \boldsymbol{\mu}_d + \Delta_d f(y) = \boldsymbol{\mu}_d + \Delta_d \mathbf{u}_y$ with \mathbf{u}_y and Δ_d satisfying the stated conditions.

Consider $K = 2$. Let $u_y = f(y) = \sqrt{\pi_2/\pi_1} \mathbb{1}\{y = 1\} - \sqrt{\pi_1/\pi_2} \mathbb{1}\{y = 2\}$, then $\mathbb{E}(u_y) = 0$, $\text{Cov}(u_y) = 1$. Setting $\Delta_d = \sqrt{\pi_1\pi_2}(\boldsymbol{\mu}_1 - \boldsymbol{\mu}_2)$ gives the desired factor model since

$$\mathbb{E}(\boldsymbol{\mu}_d + \Delta_D u_y | y = 1) = \pi_1 \boldsymbol{\mu}_1 + \pi_2 \boldsymbol{\mu}_2 + \sqrt{\pi_1\pi_2}(\boldsymbol{\mu}_1 - \boldsymbol{\mu}_2) \sqrt{\pi_2/\pi_1} = \boldsymbol{\mu}_1,$$

and similarly $\mathbb{E}(\boldsymbol{\mu}_d + \Delta_D u_y | y = 2) = \boldsymbol{\mu}_2$.

Consider $K \geq 2$. Let $\Theta \in \mathbb{R}^{K \times (K-1)}$ have columns Θ_l with

$$\Theta_l = \left(\left\{ \sqrt{\frac{\pi_{l+1}}{\sum_{i=1}^l \pi_i \sum_{i=1}^{l+1} \pi_i}} \right\}_l, -\sqrt{\frac{\sum_{i=1}^l \pi_i}{\pi_{l+1} \sum_{i=1}^{l+1} \pi_i}}, 0_{K-1-l} \right)^\top,$$

and let $\mathbf{Z} = g(y) \in \mathbb{R}^K$ be a unit norm class-indicator random vector with $z_k = 1$ if observation belongs to class k . Consider $\tilde{\mathbf{u}}_y = \tilde{f}(y) = \Theta^\top g(y) = \Theta^\top \mathbf{Z}$ and let $\boldsymbol{\pi} = (\pi_1 \dots \pi_K)^\top$. Then

$$\begin{aligned} \mathbb{E}(\tilde{\mathbf{u}}_y) &= \Theta^\top \mathbb{E}(\mathbf{Z}) = \Theta^\top \boldsymbol{\pi} = (\Theta_1^\top \boldsymbol{\pi} \dots \Theta_{K-1}^\top \boldsymbol{\pi}) = \mathbf{0}_{K-1}, \\ \text{Cov}(\tilde{\mathbf{u}}_y) &= \Theta^\top \text{Cov}(\mathbf{Z}) \Theta = \Theta^\top (\text{diag}(\boldsymbol{\pi}) - \boldsymbol{\pi} \boldsymbol{\pi}^\top) \Theta = \Theta^\top \text{diag}(\boldsymbol{\pi}) \Theta = \mathbf{I}_K. \end{aligned}$$

Next define $\tilde{\Delta}_d \in \mathbb{R}^{p \times (K-1)}$ to have columns $\tilde{\Delta}_{dr}$ with

$$\tilde{\Delta}_{dr} = \frac{\sqrt{\pi_{r+1}} \left\{ \sum_{i=1}^r \pi_i (\boldsymbol{\mu}_{di} - \boldsymbol{\mu}_{d(r+1)}) \right\}}{\sqrt{\sum_{i=1}^r \pi_i \sum_{i=1}^{r+1} \pi_i}}.$$

Then

$$\begin{aligned} \mathbb{E}(\boldsymbol{\mu}_d + \tilde{\Delta}_d \tilde{f}(y) | y = k) &= \sum_{m=1}^K \pi_m \boldsymbol{\mu}_{dm} + \tilde{\Delta}_d \boldsymbol{\Theta}^\top g(k) \\ &= \sum_{m=1}^K \pi_m \boldsymbol{\mu}_{dm} - \sqrt{\frac{\sum_{i=1}^{k-1} \pi_i}{\pi_k \sum_{i=1}^k \pi_i}} \tilde{\Delta}_{d(k-1)} + \sum_{l=k}^{K-1} \sqrt{\frac{\pi_{l+1}}{\sum_{i=1}^l \pi_i \sum_{i=1}^{l+1} \pi_i}} \tilde{\Delta}_{dl} \\ &= \boldsymbol{\mu}_{dk}, \end{aligned}$$

where in the last step we used the properties of orthogonal group-mean contrasts for unbalanced data, see [Searle \(2006\)](#) and also Proposition 2 in [Gaynanova et al. \(2016\)](#). Consider the eigendecomposition $\tilde{\Delta}_d^\top \Sigma_{dy}^{-1} \tilde{\Delta}_d = \mathbf{R}_d \Lambda_d \mathbf{R}_d^\top$. Setting $\Delta_d = \tilde{\Delta}_d \mathbf{R}_d$ and $\mathbf{u}_y = \mathbf{R}_d^\top \tilde{\mathbf{u}}_y$ leads to desired factor model. \square

Proof of Theorem 1

Proof. 1. When $q = 0$, $\Sigma_{ld} = \Delta_l \Delta_d^\top = \Sigma_l \left[\Sigma_l^{-1} \Delta_l \Delta_d^\top \Sigma_d^{-1} \right] \Sigma_d$. Let $\Lambda_d = \Delta_d^\top \tilde{\Sigma}_d^{-1} \Delta_d$, where Λ_d is diagonal by definition of factor model (4). Using Woodbury matrix identity,

$$\Delta_d^\top \Sigma_d^{-1} \Delta_d = \Delta_d^\top (\tilde{\Sigma}_d + \Delta_d \Delta_d^\top)^{-1} \Delta_d = \Lambda_d^{1/2} (\mathbf{I} + \Lambda_d)^{-1} \Lambda_d^{1/2}.$$

Let $\Theta_d = \Sigma_d^{-1} \Delta_d \Lambda_d^{-1/2} (\mathbf{I} + \Lambda_d)^{1/2}$, then $\Theta_d^\top \Sigma_d \Theta_d = \mathbf{I}$, and

$$\Sigma_{ld} = \Sigma_l \left[\Theta_l (\mathbf{I} + \Lambda_l)^{-1/2} \Lambda_l^{1/2} \Lambda_d^{1/2} (\mathbf{I} + \Lambda_d)^{-1/2} \Theta_d^\top \right] \Sigma_d = \Sigma_l \left(\sum_{k=1}^{K-1} \rho_k \boldsymbol{\theta}_l^{(k)} \boldsymbol{\theta}_d^{(k)\top} \right) \Sigma_d,$$

where ρ_k are the diagonal elements of matrix $(\mathbf{I} + \Lambda_l)^{-1/2} \Lambda_l^{1/2} \Lambda_d^{1/2} (\mathbf{I} + \Lambda_d)^{-1/2}$, and $\boldsymbol{\theta}_l^{(k)}$, $\boldsymbol{\theta}_d^{(k)}$ are corresponding columns of Θ_l , Θ_d .

2. Consider

$$\begin{aligned} \Sigma_{ld} &= \mathbf{A}_l \mathbf{A}_d^\top + \Delta_l \Delta_d^\top \\ &= \Sigma_l \left\{ \Sigma_l^{-1/2} \left(\Sigma_l^{-1/2} \mathbf{A}_l \mathbf{A}_d^\top \Sigma_d^{-1/2} + \Sigma_l^{-1/2} \Delta_l \Delta_d^\top \Sigma_d^{-1/2} \right) \Sigma_d^{-1/2} \right\} \Sigma_d \\ &= \Sigma_l \left\{ \Sigma_l^{-1/2} \left(\mathbf{R}_q \mathbf{D}_q \mathbf{P}_q^\top + \mathbf{R}_{K-1} \mathbf{D}_{K-1} \mathbf{P}_{K-1}^\top \right) \Sigma_d^{-1/2} \right\} \Sigma_d, \end{aligned}$$

where we used singular value decomposition $\Sigma_l^{-1/2} \mathbf{A}_l \mathbf{A}_d^\top \Sigma_d^{-1/2} = \mathbf{R}_q \mathbf{D}_q \mathbf{P}_q^\top$ and $\Sigma_l^{-1/2} \Delta_l \Delta_d^\top \Sigma_d^{-1/2} = \mathbf{R}_{K-1} \mathbf{D}_{K-1} \mathbf{P}_{K-1}^\top$. Since $\mathbf{A}_d^\top \tilde{\Sigma}_d^{-1} \Delta_d = \mathbf{0}$, by Woodbury matrix identity $\mathbf{A}_d^\top \Sigma_d^{-1} \Delta_d = \mathbf{0}$, and therefore $\mathbf{R}_q^\top \mathbf{R}_{K-1} = \mathbf{0}$ and $\mathbf{P}_q^\top \mathbf{P}_{K-1} = \mathbf{0}$. From the above display,

$$\Sigma_{ld} = \Sigma_l \left\{ \Sigma_l^{-1/2} \mathbf{R}_{q+K-1} \mathbf{D}_{q+K-1} \mathbf{P}_{q+K-1}^\top \Sigma_d^{-1/2} \right\} \Sigma_d.$$

The result follows by setting $\Theta_d = \Sigma_d^{-1/2} \mathbf{P}_{q+K-1}$, and using the results from part 1. \square

Proof of Proposition 2

Proof. Gaynanova et al. (2016) consider optimization problem

$$\underset{\mathbf{V} \in \mathbb{R}^{p \times (K-1)}}{\text{minimize}} \left\{ \frac{1}{2} \text{Tr}(\mathbf{V}^\top \mathbf{W} \mathbf{V}) + \frac{1}{2} \|\mathbf{D}^\top \mathbf{V} - \mathbf{I}\|_F^2 + \lambda \sum_{i=1}^p \|\mathbf{v}_i\|_2 \right\}, \quad (17)$$

where $\mathbf{W} = \frac{1}{n} \sum_{i=1}^K (n_i - 1) \mathbf{S}_i$ is the within-class sample covariance matrix, \mathbf{S}_i is the sample covariance matrix for class i and $\mathbf{D} \in \mathbb{R}^{p \times (K-1)}$ has columns \mathbf{D}_l defined as

$$\mathbf{D}_l = \frac{\sqrt{n_{l+1}} (\sum_{i=1}^l n_i (\bar{\mathbf{x}}_i - \bar{\mathbf{x}}_{l+1}))}{\sqrt{n} \sqrt{\sum_{i=1}^l n_i \sum_{i=1}^{l+1} n_i}}.$$

Here, $\bar{\mathbf{x}}_i$ is the sample mean for class i . Since $\|\mathbf{D}^\top \mathbf{V} - \mathbf{I}\|_F^2 = \text{Tr}\{(\mathbf{D}^\top \mathbf{V} - \mathbf{I})^\top (\mathbf{D}^\top \mathbf{V} - \mathbf{I})\} = \text{Tr}(\mathbf{V}^\top \mathbf{D} \mathbf{D}^\top \mathbf{V} - 2\mathbf{D}^\top \mathbf{V} + \mathbf{I})$, function (17) can be written as

$$\underset{\mathbf{V} \in \mathbb{R}^{p \times (K-1)}}{\text{minimize}} \left\{ \frac{1}{2} \text{Tr}(\mathbf{V}^\top (\mathbf{W} + \mathbf{D} \mathbf{D}^\top) \mathbf{V}) - \text{Tr}(\mathbf{D}^\top \mathbf{V}) + \lambda \sum_{i=1}^p \|\mathbf{v}_i\|_2 \right\}. \quad (18)$$

Since \mathbf{X} is centered, $\mathbf{W} + \mathbf{D} \mathbf{D}^\top = \mathbf{X}^\top \mathbf{X} / n$. By the definition of \mathbf{Z} and \mathbf{H} ,

$$\mathbf{X}^\top \mathbf{Z} = (n_1 \bar{\mathbf{x}}_1 \quad \dots \quad n_k \bar{\mathbf{x}}_k), \quad \mathbf{X}^\top \mathbf{Z} \mathbf{H} = n \mathbf{D}.$$

Plugging the above equality into (18) leads to

$$\underset{\mathbf{V} \in \mathbb{R}^{p \times (K-1)}}{\text{minimize}} \left\{ \frac{1}{2n} \text{Tr}(\mathbf{V}^\top \mathbf{X}^\top \mathbf{X} \mathbf{V}) - \frac{1}{n} \text{Tr}(\mathbf{V}^\top \mathbf{X}^\top \mathbf{Z} \mathbf{H}) + \lambda \sum_{i=1}^p \|\mathbf{v}_i\|_2 \right\}.$$

Denote $\mathbf{Z} \mathbf{H}$ by $\tilde{\mathbf{Y}}$, then the above display can be expressed as

$$\underset{\mathbf{V} \in \mathbb{R}^{p \times (K-1)}}{\text{minimize}} \left\{ \frac{1}{2n} \|\tilde{\mathbf{Y}} - \mathbf{X} \mathbf{V}\|_F^2 + \lambda \sum_{i=1}^p \|\mathbf{v}_i\|_2 \right\}.$$

\square

Proof of Lemma 1

Proof. By multiplying the covariance matrix \mathbf{G} on both sides of $\mathbf{W}_d^* \mathbf{R}_d^\top \propto \Sigma_d^{-1} \Delta_d$, it remains to show that for some orthogonal matrices \mathbf{R}_d , $\tilde{\Delta} \text{diag}(\mathbf{R}_1 \cdots, \mathbf{R}_D)^\top \propto \mathbf{G} \text{diag}(\Sigma)^{-1} \Delta$, where $\text{diag}(\Sigma)^{-1} = \text{diag}(\Sigma_1^{-1}, \dots, \Sigma_D^{-1})$. Expanding the right hand side leads to

$$\begin{aligned} \mathbf{G} \text{diag}(\Sigma)^{-1} \Delta &= \begin{pmatrix} \mathbf{I} & -\frac{1-\alpha}{D} \Sigma_{12} \Sigma_2^{-1} & \cdots & -\frac{1-\alpha}{D} \Sigma_{1D} \Sigma_D^{-1} \\ & \vdots & & \\ -\frac{1-\alpha}{D} \Sigma_{D1} \Sigma_1^{-1} & -\frac{1-\alpha}{D} \Sigma_{D2} \Sigma_2^{-1} & \cdots & \mathbf{I} \end{pmatrix} \begin{pmatrix} \Delta_1 \\ \vdots \\ \Delta_D \end{pmatrix} \\ &= \begin{pmatrix} \Delta_1 - \frac{1-\alpha}{D} \sum_{d \neq 1} \Sigma_{1d} \Sigma_d^{-1} \Delta_d \\ \vdots \\ \Delta_D - \frac{1-\alpha}{D} \sum_{d \neq D} \Sigma_{Dd} \Sigma_d^{-1} \Delta_d \end{pmatrix}. \end{aligned}$$

From the factor model decomposition (4), $\mathbf{A}_d^\top \Sigma_d^{-1} \Delta_d = 0$ holds, and hence

$$\Sigma_{ld} \Sigma_d^{-1} \Delta_d = \Delta_l \Delta_d^\top \Sigma_d^{-1} \Delta_d = \Delta_l \Lambda_d (\Lambda_d + \mathbf{I})^{-1},$$

where $\Delta_d^\top \Sigma_{dy}^{-1} \Delta_d = \Lambda_d$. It follows that

$$\Delta_l - \frac{1-\alpha}{D} \sum_{d \neq l} \Sigma_{ld} \Sigma_d^{-1} \Delta_d = \Delta_l - \frac{1-\alpha}{D} \sum_{d \neq l} \Delta_l \Lambda_d (\Lambda_d + \mathbf{I})^{-1} \propto \Delta_l.$$

Choosing \mathbf{R}_d as an orthogonal matrix such that $\tilde{\Delta}_d \mathbf{R}_d^\top = \Delta_d$ completes the proof. \square

Proof of Theorem 2

Proof. Consider the concatenated $\tilde{\mathbf{X}} = (\mathbf{X}_1 \ \mathbf{X}_2 \ \cdots \ \mathbf{X}_D)$. From Lemmas 3 and 7 in [Gaynanova \(2018\)](#), with probability at least $1 - \eta$ and some constant C

$$\left\| \frac{1}{n} \tilde{\mathbf{X}}^\top \tilde{\mathbf{X}} - \Sigma_T \right\|_\infty \leq C \tau^2 \sqrt{\frac{\log(\sum_{i=1}^D p_i \eta^{-1})}{n}},$$

where $\tau = \max_j \sqrt{\sigma_j^2 + \max_k \mu_{kj}^2}$, σ_j are diagonal elements of Σ_y and $\mu_{k,j}$ are elements of μ_k . Therefore, with probability at least $1 - \eta$

$$\|\mathbf{G} - \mathbf{X}'^\top \mathbf{X}'\|_\infty \leq \frac{1}{D} \left\| \frac{1}{n} \tilde{\mathbf{X}}^\top \tilde{\mathbf{X}} - \Sigma_T \right\|_\infty \leq \frac{C \tau^2}{D} \sqrt{\frac{\log(\sum_{i=1}^D p_i \eta^{-1})}{n}}.$$

From Lemma 5, if $s_d \leq \gamma \lambda_{\min}^2 (32D \lambda_d^2 \|\mathbf{G} - \mathbf{X}'^\top \mathbf{X}'\|_\infty)^{-1}$, then \mathbf{X}' satisfies $RE(S, 3, \boldsymbol{\lambda})$ and $\gamma \leq 2\gamma$. Hence, using $\lambda_d = C (\tau \vee \tau^2 \delta g) D^{-1} \sqrt{(K-1) \log[(K-1)p_d]/n}$, Assumption 4

and the condition $s_d^2 \log[(K-1)p_d] = o(n)$ leads to $s_d \leq \gamma \lambda_{\min}^2 (32D\lambda_d^2 \|\mathbf{G} - \mathbf{X}'^\top \mathbf{X}'\|_\infty)^{-1}$. Therefore, by Theorems 3 and 4

$$\|\widehat{\mathbf{W}} - \mathbf{W}^*\|_F = O_p \left((\tau \vee \tau^2 \delta g) \frac{1}{D\gamma} \sqrt{\frac{K-1}{n} \sum_{d=1}^D s_d \log[(K-1)p_d]} \right).$$

□

Proof of Proposition 3

Proof. By the KKT conditions (13), $\mathbf{W}_d = 0$ leads to $\mathbf{X}'_{dj}^\top \mathbf{Y}' = \lambda \mathbf{u}_{dj}$, hence by the definition of subgradient $\|\mathbf{X}'_{dj}^\top \mathbf{Y}'\|_2 = \left\| \left(\frac{\alpha \mathbf{X}_d^\top \tilde{\mathbf{Y}}}{nD} \right)_j \right\|_2 = \lambda \|\mathbf{u}_{dj}\|_2 \leq \lambda$. This implies that $\mathbf{W}_d = 0$ satisfies KKT conditions whenever $\lambda \geq \alpha(nD)^{-1} \|\mathbf{X}_d^\top \tilde{\mathbf{Y}}\|_{\infty,2}$. □

B Supporting Theorems and Lemmas

Lemma 2. Let $\phi_d = \frac{\alpha}{nD} \mathbf{X}_d^\top (\tilde{\mathbf{Y}} - \mathbf{X}_d \mathbf{W}_d^*) + \frac{1-\alpha}{nD(D-1)} \sum_{j \neq d} (\mathbf{X}_j \mathbf{W}_j^* - \mathbf{X}_d \mathbf{W}_d^*)$, and let $\widehat{\mathbf{W}}$ be the solution to (9) with $\lambda_d \geq 2 \|\mathbf{X}_d^\top \phi_d\|_{\infty,2}$. Let $\mathbf{H} = \widehat{\mathbf{W}} - \mathbf{W}^*$, and S as defined in Assumption 1, then $\mathbf{H} \in C(S, \lambda)$.

Proof. Consider the KKT conditions for (9)

$$0 = -\mathbf{X}'^\top (\mathbf{Y}' - \mathbf{X}' \widehat{\mathbf{W}}) + \widehat{\mathbf{s}},$$

where $\widehat{\mathbf{s}}_{dj} \in \partial(\lambda_d \|\mathbf{w}_{dj}\|_2)$ evaluated at $\widehat{\mathbf{W}}$. Multiplying $(\mathbf{W}^* - \widehat{\mathbf{W}})^\top$ on both sides gives

$$(\mathbf{W}^* - \widehat{\mathbf{W}})^\top \left(\mathbf{X}'^\top (\mathbf{Y}' - \mathbf{X}' \widehat{\mathbf{W}}) - \widehat{\mathbf{s}} \right) = 0.$$

Let $\Psi = \mathbf{Y}' - \mathbf{X}' \mathbf{W}^*$. Replacing \mathbf{Y}' with $\mathbf{Y}' + \mathbf{X}' \mathbf{W}^* - \mathbf{X}' \mathbf{W}^*$ and using properties of subgradient of convex functions leads to

$$\|\mathbf{X}'(\mathbf{W}^* - \widehat{\mathbf{W}})\|_F^2 \leq \langle \mathbf{X}'^\top \Psi, \widehat{\mathbf{W}} - \mathbf{W}^* \rangle + \sum_{d=1}^D \lambda_d \|\mathbf{W}_d^*\|_{1,2} - \sum_{d=1}^D \lambda_d \|\widehat{\mathbf{W}}_d\|_{1,2}.$$

Since $\langle \mathbf{X}'^\top \Psi, \widehat{\mathbf{W}} - \mathbf{W}^* \rangle = \sum_{d=1}^D \langle \mathbf{X}_d^\top \phi_d, \widehat{\mathbf{W}}_d - \mathbf{W}_d^* \rangle$, applying Hölder inequality twice and

using conditions on λ_d leads to

$$\begin{aligned}
\|\mathbf{X}'(\mathbf{W}^* - \widehat{\mathbf{W}})\|_F^2 &\leq \sum_{d=1}^D \langle \mathbf{X}_d^\top \phi_d, \widehat{\mathbf{W}}_d - \mathbf{W}_d^* \rangle + \sum_{d=1}^D \lambda_d \|\mathbf{W}_d^*\|_{1,2} - \sum_{d=1}^D \lambda_d \|\widehat{\mathbf{W}}_d\|_{1,2} \\
&\leq \sum_{d=1}^D \|\mathbf{X}_d^\top \phi_d\|_{\infty,2} \|\widehat{\mathbf{W}}_d - \mathbf{W}_d^*\|_{1,2} + \sum_{d=1}^D \lambda_d \|\mathbf{W}_d^*\|_{1,2} - \sum_{d=1}^D \lambda_d \|\widehat{\mathbf{W}}_d\|_{1,2} \\
&\leq \sum_{d=1}^D \frac{\lambda_d}{2} (\|\mathbf{H}_{d,S_d}\|_{1,2} + \|\mathbf{H}_{d,S_d^c}\|_{1,2}) + \sum_{d=1}^D \lambda_d \|\mathbf{W}_d^*\|_{1,2} - \sum_{d=1}^D \lambda_d \|\widehat{\mathbf{W}}_d\|_{1,2}.
\end{aligned}$$

Since

$$\begin{aligned}
\|\widehat{\mathbf{W}}_d\|_{1,2} &= \|\mathbf{W}_d^* + \widehat{\mathbf{W}}_d - \mathbf{W}_d^*\|_{1,2} = \|\mathbf{W}_{d,S_d}^* + \mathbf{H}_{d,S_d}\|_{1,2} + \|\mathbf{H}_{d,S_d^c}\|_{1,2} \\
&\geq \|\mathbf{W}_{d,S_d}^*\|_{1,2} - \|\mathbf{H}_{d,S_d}\|_{1,2} + \|\mathbf{H}_{d,S_d^c}\|_{1,2},
\end{aligned}$$

combining the above two displays gives

$$\|\mathbf{X}'(\mathbf{W}^* - \widehat{\mathbf{W}})\|_F^2 \leq \sum_{d=1}^D \frac{3}{2} \lambda_d \|\mathbf{H}_{d,S_d}\|_{1,2} - \sum_{d=1}^D \frac{1}{2} \lambda_d \|\mathbf{H}_{d,S_d^c}\|_{1,2}. \quad (19)$$

Since $\|\mathbf{X}'(\mathbf{W}^* - \widehat{\mathbf{W}})\|_F^2 \geq 0$, the statement follows. \square

Theorem 3. Let $\widehat{\mathbf{W}}$ be the solution to (9) with $\lambda_d \geq 2\|\mathbf{X}_d^\top \phi_d\|_{\infty,2}$, where ϕ_d are defined in Lemma 2. Under Assumption 1, if \mathbf{X}' satisfies $RE(S, \boldsymbol{\lambda})$ with $\gamma = \gamma(S, \boldsymbol{\lambda}, \mathbf{X}')$, then

$$\|\widehat{\mathbf{W}} - \mathbf{W}^*\|_F \leq \frac{3}{2\gamma} \sqrt{\sum_{d=1}^D \lambda_d^2 s_d}.$$

Proof. From equation (19), using $\mathbf{H} = \widehat{\mathbf{W}} - \mathbf{W}^*$,

$$\|\mathbf{X}'(\mathbf{W}^* - \widehat{\mathbf{W}})\|_F^2 \leq \sum_{d=1}^D \frac{3\lambda_d}{2} \|\mathbf{W}_{d,S_d}^* - \widehat{\mathbf{W}}_{d,S_d}\|_{1,2} \leq \frac{3}{2} \sum_{d=1}^D \lambda_d \sqrt{s_d} \|\mathbf{W}_{d,S_d}^* - \widehat{\mathbf{W}}_{d,S_d}\|_F.$$

Applying Cauchy-Schwartz inequality gives

$$\|\mathbf{X}'(\mathbf{W}^* - \widehat{\mathbf{W}})\|_F^2 \leq \frac{3}{2} \sqrt{\sum_{d=1}^D \lambda_d^2 s_d} \|\mathbf{W}^* - \widehat{\mathbf{W}}\|_F.$$

Since \mathbf{X}' satisfies $\text{RE}(S, \boldsymbol{\lambda})$ and $\mathbf{H} \in C(S, \boldsymbol{\lambda})$, by Lemma 2

$$\begin{aligned} \|\mathbf{W}^* - \widehat{\mathbf{W}}\|_F^2 &\leq \frac{1}{\gamma} \|\mathbf{X}'(\mathbf{W}^* - \widehat{\mathbf{W}})\|_2^2 \leq \frac{1}{\gamma} \frac{3}{2} \sqrt{\sum_{d=1}^D \lambda_d^2 s_d} \|\mathbf{W}_S^* - \widehat{\mathbf{W}}_S\|_F \\ &\leq \frac{1}{\gamma} \frac{3}{2} \sqrt{\sum_{d=1}^D \lambda_d^2 s_d} \|\mathbf{W}^* - \widehat{\mathbf{W}}\|_F. \end{aligned}$$

If $\|\mathbf{W}^* - \widehat{\mathbf{W}}\|_F^2 = 0$, the bound holds trivially. Otherwise, dividing by $\|\mathbf{W}^* - \widehat{\mathbf{W}}\|_F$ on both sides leads to the desired bound. \square

Theorem 4. *Under Assumptions 2-4, there exists $C > 0$ such that*

$$\|\mathbf{X}_d^\top \phi_d\|_{\infty, 2} \leq C (\tau \vee \tau^2 \delta g) \frac{1}{D} \sqrt{\frac{(K-1) \log((K-1) p_d \eta^{-1})}{n}}, \quad d = 1, \dots, D,$$

with probability at least $1 - \eta$, where ϕ_d are from Lemma 2.

Proof. Without loss of generality, consider $d = 1$ and let $\tilde{\boldsymbol{\Delta}} = (\tilde{\boldsymbol{\Delta}}_1^\top \quad \tilde{\boldsymbol{\Delta}}_2^\top \quad \dots \quad \tilde{\boldsymbol{\Delta}}_D^\top)^\top$, where $\tilde{\boldsymbol{\Delta}}_d \in \mathbb{R}^{p_d \times K-1}$. Applying the triangle inequality gives

$$\begin{aligned} &\|\mathbf{X}_1^\top \phi_1\|_{\infty, 2} \\ &= \left\| \frac{\alpha}{nD} \mathbf{X}_1^\top (\tilde{\mathbf{Y}} - \mathbf{X}_1 \mathbf{W}_1^*) + \frac{1-\alpha}{nD(D-1)} \sum_{l \neq 1} \mathbf{X}_1^\top (\mathbf{X}_l \mathbf{W}_l^* - \mathbf{X}_1 \mathbf{W}_1^*) \right\|_{\infty, 2} \\ &= \left\| \frac{\alpha}{nD} \mathbf{X}_1^\top (\tilde{\mathbf{Y}} - \mathbf{X}_1 \mathbf{W}_1^*) - \tilde{\boldsymbol{\Delta}}_1 + \tilde{\boldsymbol{\Delta}}_1 + \frac{1-\alpha}{nD(D-1)} \sum_{l \neq 1} \mathbf{X}_1^\top (\mathbf{X}_l \mathbf{W}_l^* - \mathbf{X}_1 \mathbf{W}_1^*) \right\|_{\infty, 2} \\ &\leq \underbrace{\left\| \frac{\alpha}{nD} \mathbf{X}_1^\top \tilde{\mathbf{Y}} - \tilde{\boldsymbol{\Delta}}_1 \right\|_{\infty, 2}}_{:=I_1} \\ &\quad + \underbrace{\left\| \tilde{\boldsymbol{\Delta}}_1 - \frac{\alpha}{nD} \mathbf{X}_1^\top \mathbf{X}_1 \mathbf{W}_1^* + \frac{1-\alpha}{nD(D-1)} \sum_{l \neq 1} \mathbf{X}_1^\top (\mathbf{X}_l \mathbf{W}_l^* - \mathbf{X}_1 \mathbf{W}_1^*) \right\|_{\infty, 2}}_{:=I_2}. \end{aligned}$$

Consider I_1 . From Lemma 4 in Gaynanova (2018), there exists $C_1 > 0$ such that

$$\left\| \frac{\alpha}{nD} \mathbf{X}_1^\top \tilde{\mathbf{Y}} - \tilde{\boldsymbol{\Delta}}_1 \right\|_{\infty, 2} \leq \frac{C_1}{D} \max_j \sigma_{1,j} \sqrt{\frac{(K-1) \log(p_1 \eta^{-1})}{n}} \leq \frac{C_1}{D} \tau \sqrt{\frac{(K-1) \log(p_1 \eta^{-1})}{n}}$$

with probability at least $1 - \eta$.

Consider I_2 .

$$\begin{aligned}
I_2 &= \left\| \tilde{\Delta}_1 - \frac{1}{n} \mathbf{X}_1^\top \left\{ \alpha \frac{1}{D} \mathbf{X}_1 \mathbf{W}_1^* + \frac{1-\alpha}{D} \mathbf{X}_1 \mathbf{W}_1^* - \frac{1-\alpha}{D(D-1)} \sum_{l \neq 1} \mathbf{X}_l \mathbf{W}_l^* \right\} \right\|_{\infty, 2} \\
&= \left\| \tilde{\Delta}_1 - \frac{1}{Dn} \mathbf{X}_1^\top \left\{ \mathbf{X}_1 \mathbf{W}_1^* - \frac{1-\alpha}{D-1} \sum_{l \neq 1} \mathbf{X}_l \mathbf{W}_l^* \right\} \right\|_{\infty, 2} \\
&= \left\| \tilde{\Delta}_1 - \frac{1}{Dn} \mathbf{X}_1^\top \mathbf{U} \right\|_{\infty, 2},
\end{aligned}$$

where $\mathbf{U} = \mathbf{X}_1 \mathbf{W}_1^* - \frac{1-\alpha}{D-1} \sum_{l \neq 1} \mathbf{X}_l \mathbf{W}_l^* \in \mathbb{R}^{n \times (K-1)}$. Since the first p_1 rows of \mathbf{G} are $(\Sigma_1 \quad -\frac{1-\alpha}{D-1} \Sigma_{12} \quad \cdots \quad -\frac{1-\alpha}{D-1} \Sigma_{1D}) / D$,

$$\begin{aligned}
\mathbb{E} \left(\frac{1}{Dn} \mathbf{X}_1^\top \mathbf{U} \right) &= \frac{1}{D} \mathbb{E} \left(\frac{1}{n} \mathbf{X}_1^\top (\mathbf{X}_1 \quad -\frac{1-\alpha}{D-1} \mathbf{X}_2 \quad \cdots \quad -\frac{1-\alpha}{D-1} \mathbf{X}_D) \mathbf{W}^* \right) \\
&= \frac{1}{D} (\Sigma_1 \quad -\frac{1-\alpha}{D-1} \Sigma_{12} \quad \cdots \quad -\frac{1-\alpha}{D-1} \Sigma_{1D}) \mathbf{G}^{-1} \tilde{\Delta} \\
&= (I_{p_1} \quad \mathbf{0}) \tilde{\Delta} = \tilde{\Delta}_1.
\end{aligned}$$

Combining the above gives

$$\begin{aligned}
I_2 &= \left\| \tilde{\Delta}_1 - \frac{1}{Dn} \mathbf{X}_1^\top \mathbf{U} \right\|_{\infty, 2} \leq \sqrt{K-1} \left\| \tilde{\Delta}_1 - \frac{1}{Dn} \mathbf{X}_1^\top \mathbf{U} \right\|_{\infty} \\
&= \sqrt{K-1} \left\| \mathbb{E} \left(\frac{1}{Dn} \mathbf{X}_1^\top \mathbf{U} \right) - \frac{1}{Dn} \mathbf{X}_1^\top \mathbf{U} \right\|_{\infty}.
\end{aligned}$$

From Lemma 3 in [Gaynanova \(2018\)](#), all elements of \mathbf{X}_1 are subgaussian with parameter at most τ . From Lemma 3, all elements of \mathbf{U} are subgaussian with parameter at most $2\tau\delta g$. Therefore, by Lemma 4, there exist $C_2 > 0$ such that with probability at least $1 - \eta$

$$I_2 \leq C_2 \frac{\tau^2 \delta g}{D} \sqrt{\frac{(K-1) \log((K-1)p_1 \eta^{-1})}{n}}.$$

Combining the results for I_1 and I_2 leads to the desired bound. \square

Lemma 3. *Under Assumptions 2-3, all elements of $\mathbf{U}_d = \mathbf{X}_d \mathbf{W}_d^* - \frac{1-\alpha}{D-1} \sum_{l \neq d} \mathbf{X}_l \mathbf{W}_l^*$, $d = 1, \dots, D$, are subgaussian with parameter $2\tau\delta g$.*

Proof. Without loss of generality, let $d = 1$ and $\mathbf{V} = (\mathbf{X}_1 \quad -\frac{1-\alpha}{D-1} \mathbf{X}_2 \quad \cdots \quad -\frac{1-\alpha}{D-1} \mathbf{X}_D) \in \mathbb{R}^{n \times \sum_{i=1}^D p_i}$ so that $\mathbf{U}_1 = \mathbf{U} = \mathbf{V} \mathbf{W}^*$. Let \mathbf{v}_i be the i^{th} row of \mathbf{V} . Under Assumptions 2-3, $\mathbf{v}_i | \mathbf{y}_i = k$ follows normal distribution with

$$\mathbb{E} [\mathbf{v}_i | \mathbf{y}_i = k] = \mathbf{P} \boldsymbol{\mu}_k, \text{Cov} [\mathbf{v}_i | \mathbf{y}_i = k] = \mathbf{P} \Sigma_y \mathbf{P} = \bar{\Sigma}_y,$$

where $\mathbf{P} = \text{diag}(\mathbf{I}_{p_1}, -\frac{1-\alpha}{D-1}\mathbf{I}_{p_2}, \dots, -\frac{1-\alpha}{D-1}\mathbf{I}_{p_D})$. Therefore,

$$\begin{aligned}\mathbf{W}^{*\top} \mathbf{v}_i &= \tilde{\Delta}^\top \mathbf{G}^{-1} \mathbf{v}_i \\ &= \tilde{\Delta}^\top \mathbf{G}^{-1} (\mathbf{P} \sum_{k=1}^K \boldsymbol{\mu}_k \mathbb{1}\{y_i = k\} + \bar{\Sigma}_y^{1/2} \mathbf{e}_i) \\ &= \tilde{\Delta}^\top \mathbf{G}^{-1} \mathbf{P} \sum_{k=1}^K \boldsymbol{\mu}_k \mathbb{1}\{y_i = k\} + \tilde{\Delta}^\top \mathbf{G}^{-1} \bar{\Sigma}_y^{1/2} \mathbf{e}_i \\ &:= \mathbf{v}_{1i} + \mathbf{v}_{2i},\end{aligned}$$

where $\mathbf{e}_i \sim \mathcal{N}(\mathbf{I})$ and $\mathbf{v}_{1i}, \mathbf{v}_{2i}$ are independent random vectors.

Let $\mathbf{M} = (\boldsymbol{\mu}_1 \ \boldsymbol{\mu}_2 \ \dots \ \boldsymbol{\mu}_K) \in \mathbb{R}^{\sum_{i=1}^D p_i \times K}$. Since $\|\mathbf{G}^{-1}\|_\infty \leq g$,

$$\begin{aligned}\|\mathbf{v}_{1i}\|_\infty &= \|\tilde{\Delta}^\top \mathbf{G}^{-1} \mathbf{P} \sum_{k=1}^K \boldsymbol{\mu}_k \mathbb{1}\{y_i = k\}\|_\infty \leq \|\tilde{\Delta}^\top \mathbf{G}^{-1} \mathbf{P} \mathbf{M}\|_{\infty,2} \\ &\leq \|\tilde{\Delta}\|_{\infty,2} \|\mathbf{G}^{-1}\|_\infty \|\mathbf{P} \mathbf{M}\|_\infty \leq \delta \tau g,\end{aligned}$$

where the second inequality is due to $\|\mathbf{A}\mathbf{B}\|_{\infty,2} \leq \|\mathbf{A}\|_\infty \|\mathbf{B}\|_{\infty,2}$ (Obozinski et al., 2011, Lemma 8). Hence all elements of \mathbf{v}_{1i} are subgaussian with parameter at most $\delta \tau g$.

On the other hand, \mathbf{v}_{2i} is a normally distributed vector with mean $\mathbf{0}$ and covariance $\text{Cov}(\mathbf{v}_{2i}) = \tilde{\Delta}^\top \mathbf{G}^{-1} \bar{\Sigma}_y \mathbf{G}^{-1} \tilde{\Delta}$. Since

$$\begin{aligned}\|\text{Cov}(\mathbf{v}_{2i})\|_\infty &= \|\tilde{\Delta}^\top \mathbf{G}^{-1} \bar{\Sigma}_y \mathbf{G}^{-1} \tilde{\Delta}\|_\infty \\ &\leq \|\tilde{\Delta}\|_\infty^2 \|\mathbf{G}^{-1}\|_\infty^2 \|\bar{\Sigma}_y\|_\infty \|\mathbf{P}\|_\infty^2 \\ &\leq \|\tilde{\Delta}\|_{\infty,2}^2 \|\mathbf{G}^{-1}\|_\infty^2 \|\bar{\Sigma}_y\|_\infty \leq \delta^2 \tau^2 g^2,\end{aligned}$$

all elements of \mathbf{v}_{2i} are also subgaussian with parameter $\delta \tau g$.

Combining the results for \mathbf{v}_{1i} and \mathbf{v}_{2i} ,

$$\mathbb{E}(e^{\lambda u_{ij}}) = \mathbb{E}\{e^{\lambda(v_{1ij} + v_{2ij})}\} = \mathbb{E}(e^{\lambda v_{1ij}}) \mathbb{E}(e^{\lambda v_{2ij}}) \leq e^{\lambda^2 \{2\tau \delta g\}^2 / 2}.$$

This implies that all elements of \mathbf{U}_1 are subgaussian with parameter $2\tau \delta g$. \square

Lemma 4. Let $(\mathbf{x}_i, \mathbf{y}_i) \in \mathbb{R}^p \times \mathbb{R}^q$ be independent identically distributed pairs of mean zero random vectors with $\mathbb{E}(\mathbf{x}_i \mathbf{y}_i^\top) = \Sigma_{xy}$, and let all elements of \mathbf{x}_i and \mathbf{y}_i be sub-gaussian with parameters τ_1 and τ_2 , respectively. Let $\mathbf{X} = [\mathbf{x}_1 \dots \mathbf{x}_n]^\top$, $\mathbf{Y} = [\mathbf{y}_1 \dots \mathbf{y}_n]^\top$. If $\log(pq) = o(n)$, then with probability at least $1 - \eta$ for some constant $C > 0$

$$\left\| \frac{1}{n} \mathbf{X}^\top \mathbf{Y} - \Sigma_{xy} \right\|_\infty \leq C \tau_1 \tau_2 \sqrt{\frac{\log(pq/\eta)}{n}}.$$

Proof. Let $u_{ikj} = x_{ji}y_{jk}$, then u_{ikj} is sub-exponential with parameter $2\tau_1\tau_2$ (Vershynin, 2012, Lemma 5.14). Let σ_{ik} be elements of Σ_{xy} , then $u_{ikj} - \sigma_{ik}$ are sub-exponential with parameter $4\tau_1\tau_2$, and using Bernstein's bound (Vershynin, 2012, Proposition 5.16)

$$\text{pr} \left(\left\| \frac{1}{n} \sum_{j=1}^n u_{ikj} - \sigma_{ik} \right\|_{\infty} \geq \varepsilon \right) \leq 2 \exp \left\{ -C \min \left(\frac{\varepsilon^2}{16\tau_1^2\tau_2^2}, \frac{\varepsilon}{4\tau_1\tau_2} \right) n \right\}$$

for some $C > 0$. By union bound

$$\text{pr}(\|\mathbf{X}^{\top} \mathbf{Y}/n - \Sigma\|_{\infty} \geq \varepsilon) \leq pq \text{pr} \left(\left\| \frac{1}{n} \sum_{j=1}^n u_{ikj} - \sigma_{ik} \right\|_{\infty} \geq \varepsilon \right).$$

Setting $\varepsilon = C_1\tau_1\tau_2\sqrt{\frac{\log(pq/\eta)}{n}}$ and using $\log(pq) = o(n)$ completes the proof. \square

Lemma 5. *Let $\mathbf{G}^{1/2}$ satisfy $RE(S, \boldsymbol{\lambda})$ with $\gamma = \gamma(S, \boldsymbol{\lambda}, \mathbf{G}^{1/2})$, and let $\lambda_{\min} := \min_{d=1, \dots, D} \lambda_d$. If $s_d \leq \gamma \lambda_{\min}^2 (32D\lambda_d^2 \|\mathbf{G} - \mathbf{X}'^{\top} \mathbf{X}'\|_{\infty})^{-1}$, then \mathbf{X}' satisfies $RE(S, \boldsymbol{\lambda})$ and*

$$0 < \gamma(S, \boldsymbol{\lambda}, \mathbf{X}') \leq 2\gamma(S, \boldsymbol{\lambda}, \mathbf{G}^{1/2}).$$

Proof. Since $\mathbf{G}^{1/2}$ satisfies $RE(S, \boldsymbol{\lambda})$, for all $\mathbf{A} \in \mathcal{C}(S, \boldsymbol{\lambda})$

$$\text{Tr}(\mathbf{A}^{\top} \mathbf{X}'^{\top} \mathbf{X}' \mathbf{A}) = \text{Tr}(\mathbf{A}^{\top} \mathbf{G} \mathbf{A}) + \text{Tr}\{\mathbf{A}^{\top} (\mathbf{G} - \mathbf{X}'^{\top} \mathbf{X}') \mathbf{A}\} \geq \gamma \|\mathbf{A}\|_F^2 - \|\mathbf{A}\|_{1,2}^2 \|\mathbf{G} - \mathbf{X}'^{\top} \mathbf{X}'\|_{\infty}.$$

Since $\mathbf{A} \in \mathcal{C}(S, \boldsymbol{\lambda})$, we have

$$\begin{aligned} \|\mathbf{A}\|_{1,2} &\leq \sum_{d=1}^D \frac{\lambda_d}{\lambda_{\min}} (\|\mathbf{A}_{d,S_d}\|_{1,2} + \|\mathbf{A}_{d,S_d^c}\|_{1,2}) \\ &\leq 4 \sum_{d=1}^D \frac{\lambda_d}{\lambda_{\min}} \|\mathbf{A}_{d,S_d}\|_{1,2} \leq 4 \sum_{d=1}^D \sqrt{s_d} \frac{\lambda_d}{\lambda_{\min}} \|\mathbf{A}_{d,S_d}\|_F \\ &\leq 4 \sqrt{\frac{\sum_{d=1}^D \lambda_d^2 s_d}{\lambda_{\min}^2}} \|\mathbf{A}_S\|_F \leq 4 \sqrt{\frac{\sum_{d=1}^D \lambda_d^2 s_d}{\lambda_{\min}^2}} \|\mathbf{A}\|_F, \end{aligned}$$

Therefore

$$\begin{aligned} \text{Tr}(\mathbf{A}^{\top} \mathbf{X}'^{\top} \mathbf{X}' \mathbf{A}) &\geq \gamma \|\mathbf{A}\|_F^2 - 16 \frac{\sum_{d=1}^D \lambda_d^2 s_d}{\lambda_{\min}^2} \|\mathbf{A}\|_F^2 \|\mathbf{G} - \mathbf{X}'^{\top} \mathbf{X}'\|_{\infty} \\ &\geq \gamma \|\mathbf{A}\|_F^2 - \frac{\gamma}{2} \|\mathbf{A}\|_F^2 = \frac{\gamma}{2} \|\mathbf{A}\|_F^2, \end{aligned}$$

where the last inequality holds because of the condition on s_d . \square

C Regression formulation via augmented data approach

In this section, we reformulate (8) as a regression problem using augmented data approach. Let $\mathbf{W} = (\mathbf{W}_1^\top, \dots, \mathbf{W}_D^\top)^\top$,

$$\mathbf{X}' = \begin{pmatrix} \sqrt{\alpha}\mathbf{X}_1 & \mathbf{0} & \mathbf{0} & \dots & \mathbf{0} \\ \mathbf{0} & \sqrt{\alpha}\mathbf{X}_2 & \mathbf{0} & \dots & \mathbf{0} \\ & & \vdots & & \\ \mathbf{0} & \mathbf{0} & \mathbf{0} & \dots & \sqrt{\alpha}\mathbf{X}_D \\ \sqrt{\frac{1-\alpha}{D-1}}\mathbf{X}_1 & -\sqrt{\frac{1-\alpha}{D-1}}\mathbf{X}_2 & \mathbf{0} & \dots & \mathbf{0} \\ \sqrt{\frac{1-\alpha}{D-1}}\mathbf{X}_1 & \mathbf{0} & -\sqrt{\frac{1-\alpha}{D-1}}\mathbf{X}_3 & \dots & \mathbf{0} \\ \sqrt{\frac{1-\alpha}{D-1}}\mathbf{X}_1 & \mathbf{0} & \mathbf{0} & \dots & -\sqrt{\frac{1-\alpha}{D-1}}\mathbf{X}_D \\ & & \vdots & & \\ \mathbf{0} & \mathbf{0} & \dots & \sqrt{\frac{1-\alpha}{D-1}}\mathbf{X}_{D-1} & -\sqrt{\frac{1-\alpha}{D-1}}\mathbf{X}_D \end{pmatrix} / \sqrt{nD},$$

$$\mathbf{Y}' = \sqrt{\frac{\alpha}{nD}} \left(\underbrace{\tilde{\mathbf{Y}}^\top \dots \tilde{\mathbf{Y}}^\top}_D \mathbf{0} \dots \mathbf{0} \right)^\top.$$

Then (8) is equivalent to

$$\underset{\mathbf{W}}{\text{minimize}} \left\{ 2^{-1} \|\mathbf{Y}' - \mathbf{X}'\mathbf{W}\|_F^2 + \sum_{d=1}^D \lambda_d \text{Pen}(\mathbf{W}_d) \right\}.$$

D Variable selection comparison

We use precision and recall to compare the methods in terms of variable selection. Let \mathbf{A}_d be the set of nonzero rows of Θ_d , and let $\widehat{\mathbf{A}}_d$ be the set of nonzero rows in $\widehat{\mathbf{W}}_d$. Let $\#\{\mathbf{A}_d\}$ denote the cardinality of \mathbf{A}_d . We define the precision and recall as

$$\text{Precision}(\mathbf{W}_d) = \frac{\#\{\mathbf{A}_d \cap \widehat{\mathbf{A}}_d\}}{\#\{\widehat{\mathbf{A}}_d\}} \quad \text{and} \quad \text{Recall}(\mathbf{W}_d) = \frac{\#\{\mathbf{A}_d \cap \widehat{\mathbf{A}}_d\}}{\#\{\mathbf{A}_d\}}.$$

D.1 Two datasets, two groups

We consider the simulation setting from Section 6.3, the values of precision and recall for different methods are reported in Figure 4. Overall, JACA achieves the best trade off between precision and recall. JACA's precision is second best to SLDA_joint, but SLDA_joint has the lowest values of recall. JACA's recall is comparable to SLDA_sep and worse than the recall of sparse CCA methods, but the latter has low values of precision.

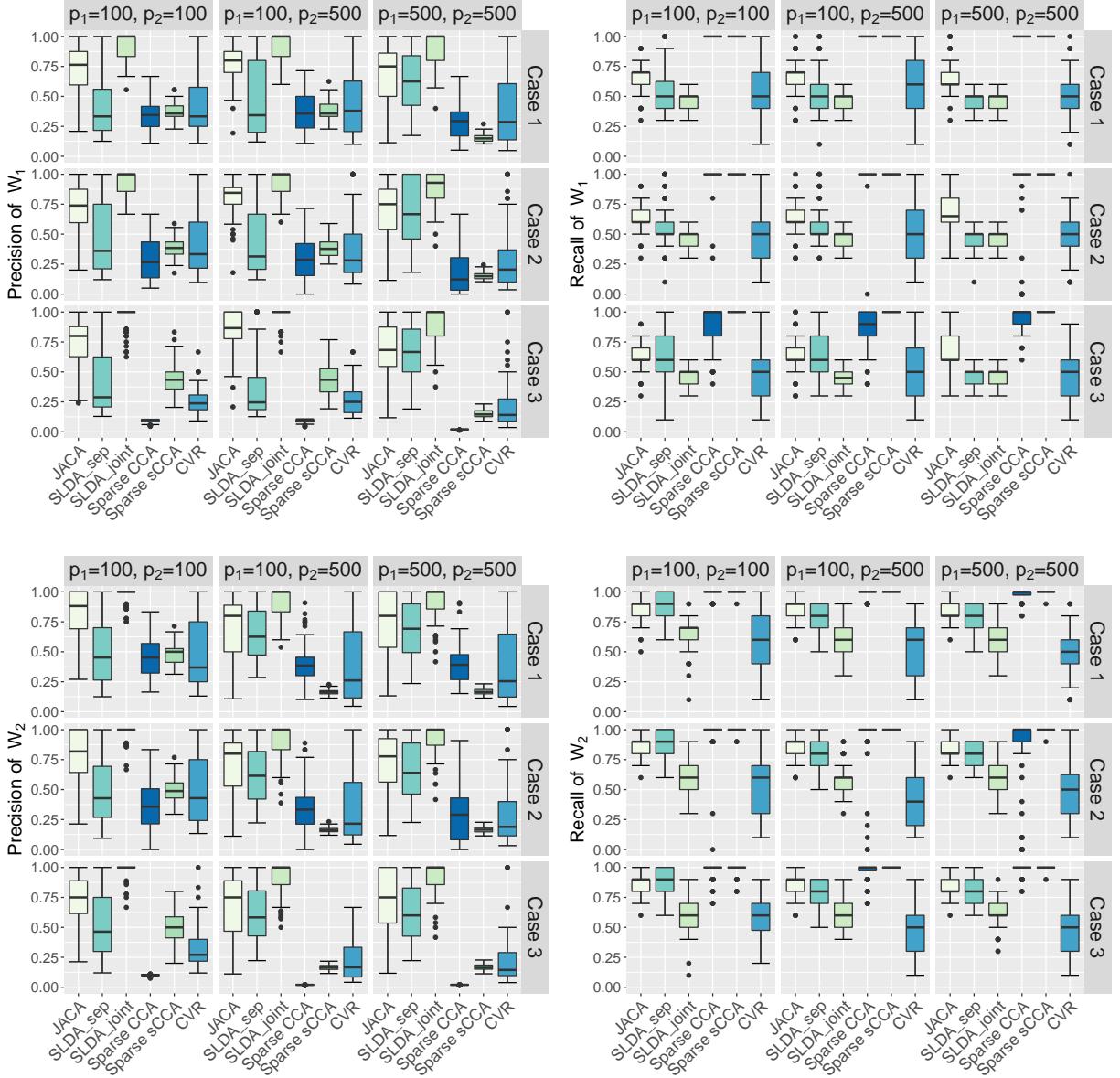


Figure 4: Precision and Recall over 100 replications when $D = 2$ and $K = 2$.

D.2 Multiple datasets, multiple groups

We consider the simulation setting from Section 6.4, the values of precision and recall for different methods are reported in Figure 5, and the conclusions are similar to the case of two-groups and two-views. Overall, JACA achieves the best trade off between precision and recall.

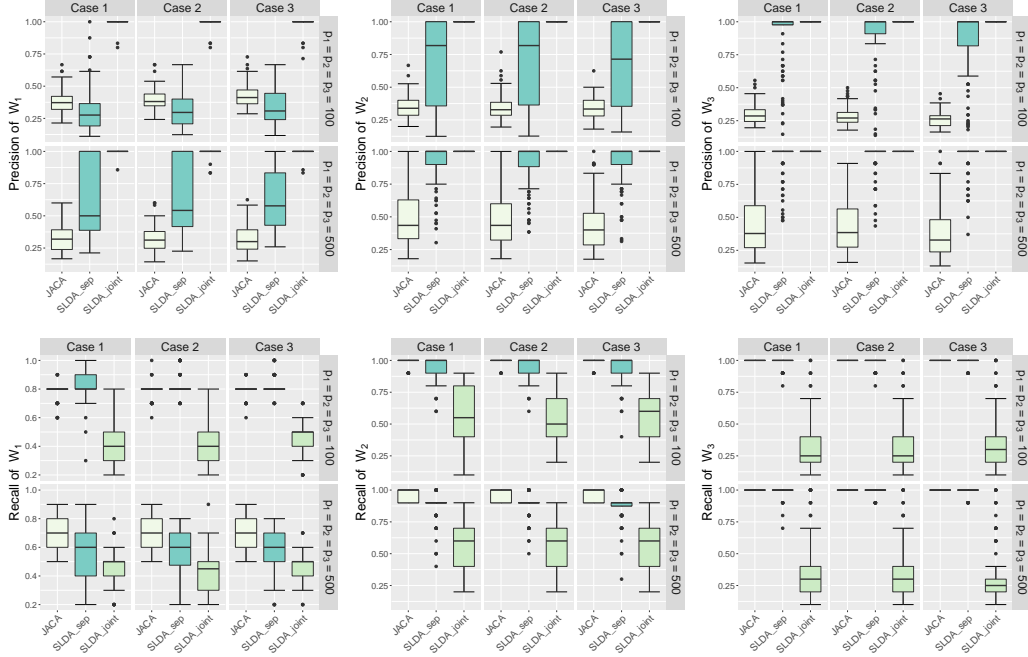


Figure 5: Precision and Recall over 100 replications when $D = 3$ and $K = 3$.

D.3 JACA versus semi-supervised JACA

In Figure 6 we compare the variable selection performance of JACA with semi-supervised JACA (ssJACA) using the setting from Section 6.3. The average performance of both approaches is similar, with ssJACA having lower variability across the replications.

E Additional data analysis

E.1 TCGA-COAD data

In this section we present additional results from the analysis of COAD data from Section 7. The enlarged heatmaps from Figure 3 are displayed in Figure 7.

We also consider the visual separation of subtypes based on the projection of RNAseq and miRNA data using discriminant directions found by JACA and ssJACA (Figure 8). The triangular points in transparent colors indicate 167 subjects with complete view and subtype information. The round points in solid colors are subjects who have missing subtypes, but for whom the subtypes have been previously predicted using random forest classifier (Guinney et al., 2015). We treat these predictions as the gold standard. The square points in solid colors are subjects with no assigned subtype, which are deemed to have mixed subtype membership (Guinney et al., 2015). The subtype separation is clear based on the projected

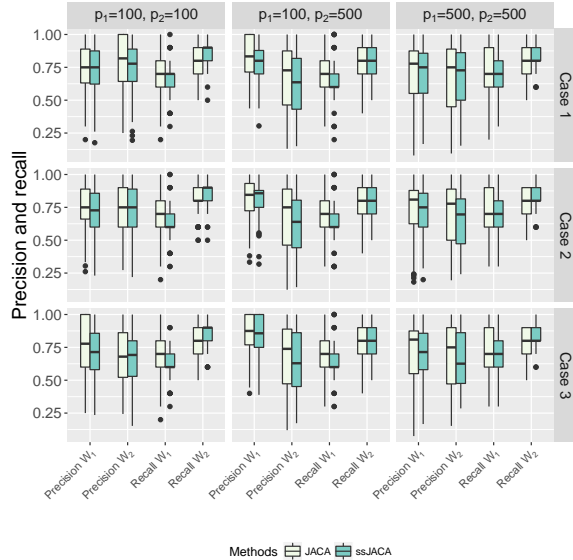


Figure 6: Comparison between JACA and semi-supervised JACA (ssJACA) over 100 replications when $D = 2$, $K = 2$. JACA uses $n = 100$ samples with complete view/class information, whereas ssJACA uses extra 100 samples with missing class information.

values, with square points being often in the middle of other subtypes, thus confirming the possibility of mixed subtype membership for those subjects.

E.2 TCGA-BRCA dataset

We consider breast cancer data from The Cancer Genome Atlas project with 4 views: gene expression (GE), DNA methylation (ME), miRNA expression (miRNA), and reverse phase protein array (RPPA). The samples are separated into 4 breast cancer subtypes: Basal, LumA, LumB and Her2 ([The Cancer Genome Atlas Network, 2012](#)). Five samples are labelled as Normal-like, and we exclude them from the analyses. [Li et al. \(2016\)](#) incorporate subtypes into supervised singular value decomposition, however only GE view is considered. [Lock and Dunson \(2013\)](#) and [Gaynanova and Li \(2017\)](#) jointly analyze all views, however do not take advantage of the subtypes. In this section, we apply JACA to understand the subtype-driven relationships between the views. We use data from https://tcga-data.nci.nih.gov/docs/publications/brca_2012 and the same data-processing as in [Lock and Dunson \(2013\)](#). While the combined number of subjects is 792, only 377 have complete view/subtype information (see [Table 9](#)).

First, we compare JACA with SLDA_sep and SLDA_joint on the 377 subjects with complete view/subtype information following the same strategy as in [Section 7](#). We do not consider CVR due to $K > 2$ and $D > 2$, and we do not consider Sparse CCA or Sparse sCCA due to their poor performance on COAD data. [Tables 10 and 11](#) display the mean

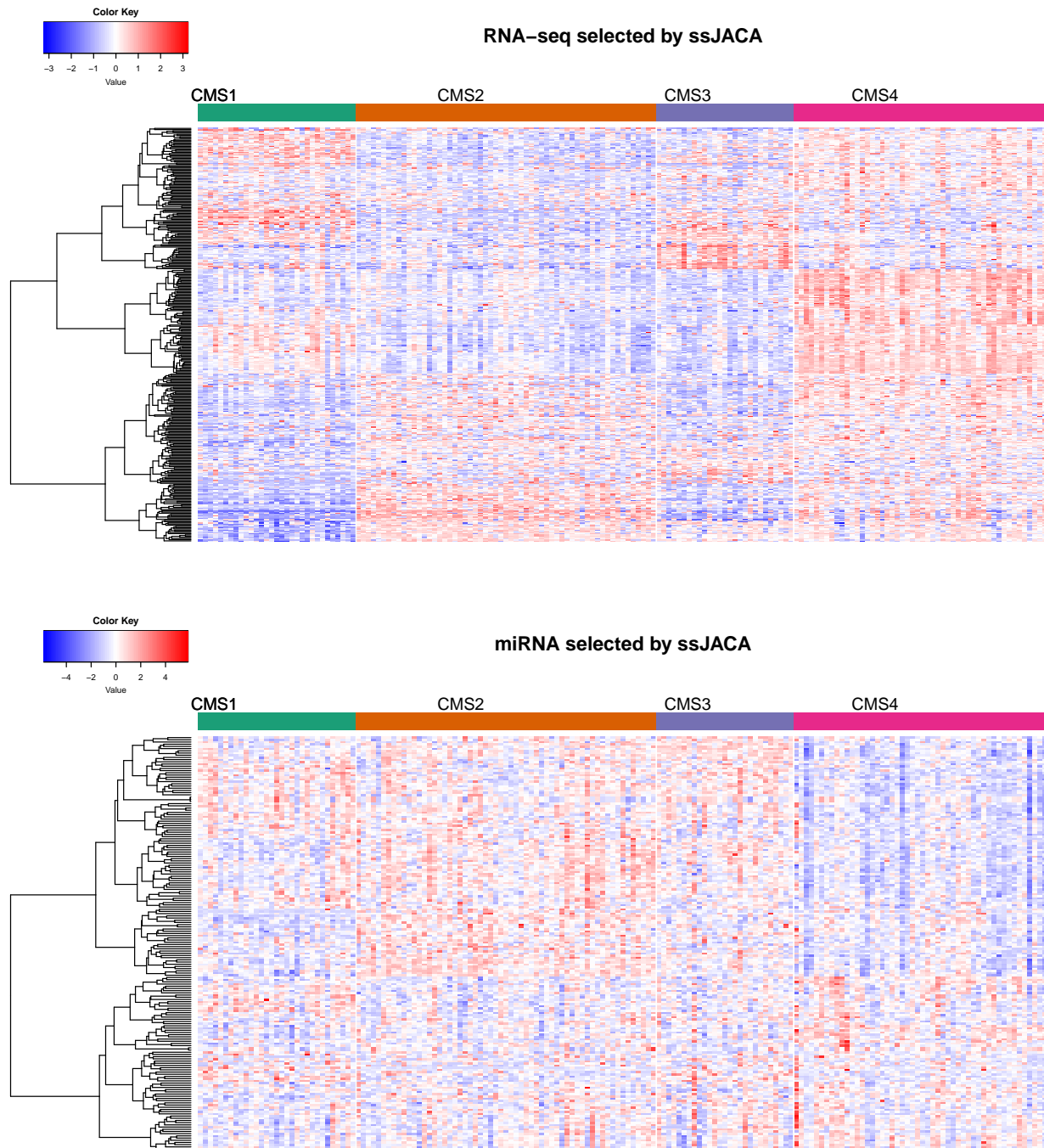


Figure 7: Heatmaps of RNaseq and miRNA views from COAD data based on features selected by ssJACA. We use Ward's linkage with euclidean distances for feature ordering.

misclassification error rates and the number of selected variables for each view, where the

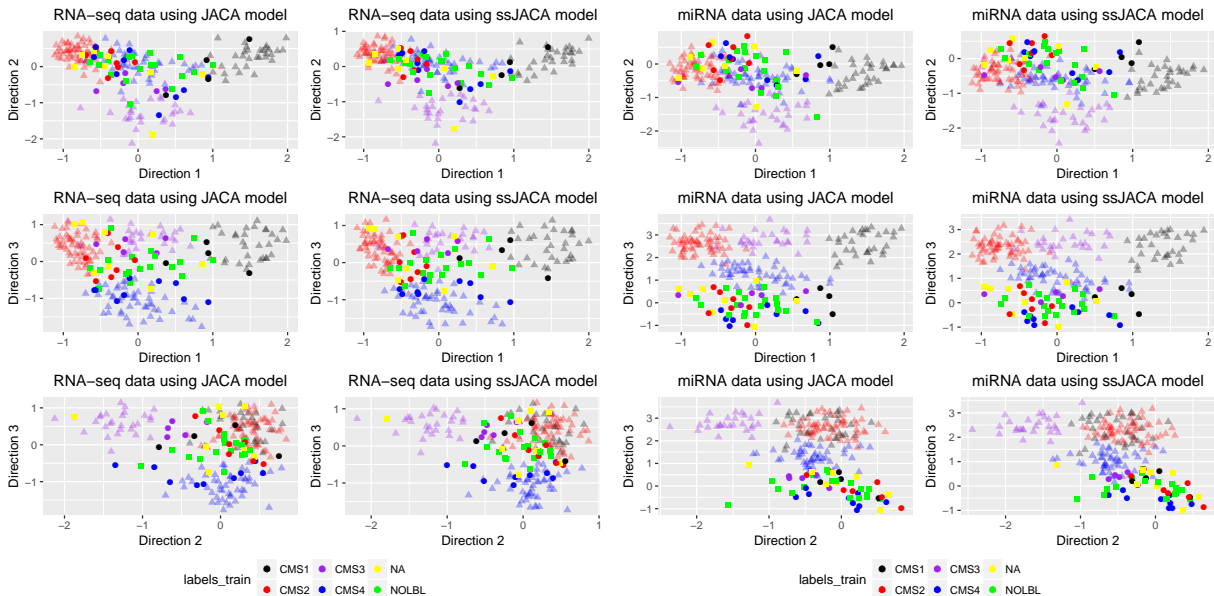


Figure 8: Projection of RNaseq and miRNA views from COAD data onto discriminant directions found by JACA and ssJACA.

GE	ME	miRNA	RPPA	Cancer type	Count
yes	yes	yes	yes	yes	377
yes	yes	yes	no	yes	114
yes	yes	no	yes	yes	19
yes	yes	no	no	yes	3
yes	no	yes	yes	yes	1
no	yes	yes	yes	no	1
no	yes	yes	no	no	193
no	yes	no	no	no	84
					Total = 792

Table 9: Number of samples in BRCA data with different missing patterns of views and cancer subtype. There are only 377 samples with complete information, whereas semi-supervised JACA approach allows to use 708 (all except the last row).

predictions are made either separately on each view, or jointly using all views. The results are similar to Section 7. The error rates are higher when using ME, miRNA or RPPA compared to GE, which is not surprising since BRCA subtypes are originally determined based on gene expression. SLDA_joint achieves a similar error rate using GE alone and higher error rates when using other views. The reason is that it selects very few variables from other views since the subtype-specific signal is the strongest in GE view. JACA has similar performance with SLDA_sep using GE, but outperforms SLDA_sep on other views, which suggests the advantage of taking into account the associations between the views. JACA

Method	Misclassification Rate (%)				
	GE	ME	miRNA	RPPA	All
JACA	10.17 (0.34)	16.65 (0.51)	16.4 (0.41)	21.76 (0.43)	13.54 (0.42)
SLDA_sep	10.15 (0.42)	20.32 (0.73)	17.32 (0.49)	23.4 (0.46)	12.4 (0.44)
SLDA_joint	10.77 (0.36)	51.33 (1.11)	54.95 (1.52)	42.4 (1.04)	10.79 (0.36)

Table 10: Mean misclassification error rates over 100 splits of 377 samples from BRCA data, standard errors are given in brackets and the lowest values are highlighted in bold.

Method	Cardinality				
	GE	ME	miRNA	RPPA	All
JACA	183.2 (1.8)	191.6 (2)	129.7 (1.5)	82.2 (0.7)	374.8 (3.6)
SLDA_sep	62.8 (2.8)	85.8 (4.5)	48.6 (2.4)	27.2 (1.8)	148.6 (5.6)
SLDA_joint	48.1 (2.3)	2.6 (0.3)	1.8 (0.2)	3.4 (0.2)	50.7 (2.5)

Table 11: Mean numbers of selected features over 100 splits of 377 samples from BRCA data, standard errors are given in brackets and the lowest values are highlighted in bold.

	JACA	SLDA_sep	SLDA_joint
Correlation	5.54 (0.01)	5.06 (0.014)	1.26 (0.057)

Table 12: Analysis based on 377 samples from BRCA data with complete view and subtype information based on 100 random splits. Mean correlation between $\mathbf{X}_1 \widehat{\mathbf{W}}_1$ and $\mathbf{X}_2 \widehat{\mathbf{W}}_2$ where $\mathbf{X}_1, \mathbf{X}_2$ are samples from test data, and $\widehat{\mathbf{W}}_1, \widehat{\mathbf{W}}_2$ are estimated from the training data, standard errors are given in brackets and the highest value is highlighted in bold.

also has higher cardinality, which is consistent with simulation results in Section 6. Table 12 displays the sum correlation, with JACA performing best compared to SLDA methods.

We further compare JACA fitted on 377 subjects (all views available) with ssJACA fitted on 708 (at least two views available). In Table 13 we compare in-sample misclassification errors based on (i) 377 samples with complete information; and (ii) additional 137 samples for which GE and class information is available, but at least one other view is missing. On 377 samples, ssJACA misclassification rates are better based on GE and ME data, but are somewhat worse for miRNA and RPPA. On 137 samples, ssJACA has a much better performance, likely because ssJACA can incorporate the information from those sample within the estimation procedure. Table 14 compares the number of features selected by both methods. ssJACA tends to select more variables than JACA, with a significant overlap between the two.

Method	out of 377 subjects					out of 137 subjects
	GE	ME	miRNA	RPPA	All	GE
JACA	23	40	38	65	34	13
ssJACA	19	38	39	72	33	6

Table 13: Number of misclassified samples on BRCA data. JACA uses 377 subjects and ssJACA is uses 708 subjects. Second to sixth columns correspond to 377 subjects with complete information, whereas the last column corresponds to 137 subject with GE and subtype information, but at least one other view missing.

	GE	ME	miRNA	RPPA
JACA	465	393	299	129
ssJACA	579	457	318	135
Intersection	394	371	277	128

Table 14: Cardinality comparison of JACA and ssJACA on BRCA data. JACA is trained using 377 subjects and ssJACA is trained using 708 subjects. The third row is the numbers of features shared by both methods.

References

- Boyd, S. P. and Vandenberghe, L. (2004). *Convex Optimization*. Cambridge Univ Press, Cambridge.
- Chen, M., Gao, C., Ren, Z., and Zhou, H. H. (2013). Sparse cca via precision adjusted iterative thresholding. *arXiv preprint arXiv:1311.6186*.
- Gao, C., Ma, Z., and Zhou, H. H. (2017). Sparse CCA: Adaptive estimation and computational barriers. *Annals of Statistics*, 45(5):2074–2101.
- Gaynanova, I. (2016). *MGSDA: Multi-Group Sparse Discriminant Analysis*. R package version 1.4.
- Gaynanova, I. (2018). Prediction and estimation consistency of sparse multi-class penalized optimal scoring. *arXiv.org*, page arXiv:1809.04669.
- Gaynanova, I., Booth, J. G., and Wells, M. T. (2016). Simultaneous sparse estimation of canonical vectors in the $p \gg N$ setting. *Journal of the American Statistical Association*, 111(514):696–706.
- Gaynanova, I. and Kolar, M. (2015). Optimal variable selection in multi-group sparse discriminant analysis. *Electronic Journal of Statistics*, 9(2):2007–2034.
- Gaynanova, I. and Li, G. (2017). Structural learning and integrative decomposition of multi-view data. *arXiv.org*.

- Gross, S. M. and Tibshirani, R. J. (2015). Collaborative regression. *Biostatistics*, 16(2):326–338.
- Guinney, J., Dienstmann, R., Wang, X., De Reyniès, A., Schlicker, A., Soneson, C., Marisa, L., Roepman, P., Nyamundanda, G., Angelino, P., et al. (2015). The consensus molecular subtypes of colorectal cancer. *Nature Medicine*, 21(11):1350–1356.
- Hastie, T. J., Tibshirani, R. J., and Buja, A. (1994). Flexible discriminant analysis by optimal scoring. *Journal of the American Statistical Association*, 89(428):1255–1270.
- Hastie, T. J., Tibshirani, R. J., and Wainwright, M. J. (2015). *Statistical Learning with Sparsity. The Lasso and Generalizations*. CRC Press.
- Hebiri, M. and Van De Geer, S. A. (2011). The Smooth-Lasso and other $\ell_1 + \ell_2$ -penalized methods. *Electronic Journal of Statistics*, 5:1184–1226.
- Li, G. and Jung, S. (2017). Incorporating covariates into integrated factor analysis of multi-view data. *Biometrics*, 73(4):1433–1442.
- Li, G., Yang, D., Nobel, A. B., and Shen, H. (2016). Supervised singular value decomposition and its asymptotic properties. *Journal of Multivariate Analysis*, 146:7–17.
- Li, Y. and Jia, J. (2017). L1 least squares for sparse high-dimensional LDA. *Electronic Journal of Statistics*, 11(1):2499–2518.
- Lock, E. F. and Dunson, D. B. (2013). Bayesian consensus clustering. *Bioinformatics*, 29(20):2610–2616.
- Lounici, K., Pontil, M., Van De Geer, S. A., and Tsybakov, A. B. (2011). Oracle inequalities and optimal inference under group sparsity. *Annals of Statistics*, 39(4):2164–2204.
- Luo, C. and Chen, K. (2017). *CVR: Canonical Variate Regression*. R package version 0.1.1.
- Luo, C., Liu, J., Dey, D. K., and Chen, K. (2016). Canonical variate regression. *Biostatistics*, 17(3):468–483.
- Mardia, K. V., Kent, J. T., and Bibby, J. M. (1979). *Multivariate Analysis*. Academic Press Inc.
- Nardi, Y. and Rinaldo, A. (2008). On the asymptotic properties of the group lasso estimator for linear models. *Electronic Journal of Statistics*, 2(0):605–633.
- Obozinski, G., Wainwright, M. J., and Jordan, M. I. (2011). Support union recovery in high-dimensional multivariate regression. *Annals of Statistics*, 39(1):1–47.
- Robert, P. and Escoufier, Y. (1976). A unifying tool for linear multivariate statistical methods: The rv- coefficient. *Journal of the Royal Statistical Society, Ser. C*, 25(3):257–265.

- Rudelson, M. and Zhou, S. (2013). Reconstruction from anisotropic random measurements. *IEEE Transactions on Information Theory*, 59(6):3434–3447.
- Searle, S. R. (2006). *Linear Models for Unbalanced Data*. Wiley-Interscience.
- The Cancer Genome Atlas Network (2012). Comprehensive molecular portraits of human breast tumours. *Nature*, 490(7418):61.
- Tseng, P. (2001). Convergence of a block coordinate descent method for nondifferentiable minimization. *Journal of Optimization Theory and Applications*, 109(3):475–494.
- Vershynin, R. (2012). Introduction to the non-asymptotic analysis of random matrices. In *Compressed Sensing*, pages 210–268. Cambridge Univ. Press, Cambridge.
- Wan, Y. W., Allen, G. I., and Liu, Z. (2015). TCGA2STAT: simple TCGA data access for integrated statistical analysis in R. *Bioinformatics*, 32(6):952–954.
- Weinstein, J. N., Collisson, E. A., Mills, G. B., Shaw, K. R. M., Ozenberger, B. A., Ellrott, K., Shmulevich, I., Sander, C., Stuart, J. M., Cancer Genome Atlas Research Network, et al. (2013). The cancer genome atlas pan-cancer analysis project. *Nature Genetics*, 45(10):1113.
- Witten, D., Tibshirani, R., Gross, S., and Narasimhan, B. (2013). *PMA: Penalized Multivariate Analysis*. R package version 1.0.9.
- Witten, D. M. and Tibshirani, R. J. (2009). Extensions of sparse canonical correlation analysis with applications to genomic data. *Statistical Applications in Genetics and Molecular Biology*, 8(1):1–27.
- Witten, D. M., Tibshirani, R. J., and Hastie, T. J. (2009). A penalized matrix decomposition, with applications to sparse principal components and canonical correlation analysis. *Biostatistics*, 10(3):515–534.
- Zou, H. and Hastie, T. J. (2005). Regularization and variable selection via the elastic net. *Journal of the Royal Statistical Society, Ser. B*, 67(2):301–320.